

การวัดปริมาณรังสีของผู้ป่วยในการตรวจรักษาด้วยวิธีทีเอชอี (TACE) และการตรวจรักษา
ทางเดินน้ำดีโดยวิธีพีทีบีดี (PTBD) โดยใช้เครื่อง มิคซอฟ ในการตรวจวัด



นางสาวสายวรุณ เทียนเครือ

จุฬาลงกรณ์มหาวิทยาลัย

CHULALONGKORN UNIVERSITY

บทคัดย่อและแฟ้มข้อมูลฉบับเต็มของวิทยานิพนธ์ตั้งแต่ปีการศึกษา 2554 ที่ให้บริการในคลังปัญญาจุฬาฯ (CUIR)
เป็นแฟ้มข้อมูลของนิสิตเจ้าของวิทยานิพนธ์ ที่ส่งผ่านทางบัณฑิตวิทยาลัย

The abstract and full text of theses from the academic year 2011 in Chulalongkorn University Intellectual Repository (CUIR)
are the thesis authors' files submitted through the University Graduate School.

วิทยานิพนธ์นี้เป็นส่วนหนึ่งของการศึกษาตามหลักสูตรปริญญาวิทยาศาสตรมหาบัณฑิต

สาขาวิชาอายุเวชศาสตร์ ภาควิชารังสีวิทยา

คณะแพทยศาสตร์ จุฬาลงกรณ์มหาวิทยาลัย

ปีการศึกษา 2559

ลิขสิทธิ์ของจุฬาลงกรณ์มหาวิทยาลัย

Patient Dose Measurement in TACE and PTBD Procedures
Using Scintillation with Optical Fiber Dosimeter

Miss Saiwaroon Teankuae



A Thesis Submitted in Partial Fulfillment of the Requirements
for the Degree of Master of Science Program in Medical Imaging
Department of Radiology
Faculty of Medicine
Chulalongkorn University
Academic Year 2016
Copyright of Chulalongkorn University

Thesis Title	Patient Dose Measurement in TACE and PTBD Procedures Using Scintillation with Optical Fiber Dosimeter
By	Miss Saiwaroon Teankuae
Field of Study	Medical Imaging
Thesis Advisor	Associate Professor Anchali Krisanachinda, Ph.D.
Thesis Co-Advisor	Professor Masayori Ishikawa, Ph.D.

Accepted by the Faculty of Medicine, Chulalongkorn University in Partial Fulfillment of the Requirements for the Master's Degree

..... Dean of the Faculty of Medicine
(Professor Suttipong Wacharasindhu, M.D.)

THESIS COMMITTEE

..... Chairman
(Assistant Professor Jarturon Tantivatana, M.D.)

..... Thesis Advisor
(Associate Professor Anchali Krisanachinda, Ph.D.)

..... Thesis Co-Advisor
(Professor Masayori Ishikawa, Ph.D.)

..... External Examiner
(Professor Franco Milano, Ph.D.)

..... External Examiner
(Professor Kosuke Matsubara, Ph.D.)

สาขารุณ เทียนเครือ : การวัดปริมาณรังสีของผู้ป่วยในการตรวจรักษาด้วยวิธีทีเอซีอี (TACE) และการตรวจรักษาทางเดินน้ำดีโดยวิธีพีทีบีดี (PTBD) โดยใช้เครื่อง มิคซอฟ ในการตรวจวัด (Patient Dose Measurement in TACE and PTBD Procedures Using Scintillation with Optical Fiber Dosimeter) อ.ที่ปรึกษาวิทยานิพนธ์หลัก: รศ. ดร. อัญชลี กฤษณจินดา, อ.ที่ปรึกษาวิทยานิพนธ์ร่วม: ศ. ดร. มาซาโยริ อิชิกาวา, 97 หน้า.

การวัดปริมาณรังสีที่ผิวหนังโดยใช้เครื่องมิคซอฟ (MIDSOF) ที่เป็นซินทิลเลเตอร์ มีความเหมาะสมและสะดวก ผู้ป่วยที่ได้รับการตรวจรักษาด้วยวิธีทีเอซีอี (TACE) และการตรวจรักษาทางเดินน้ำดีโดยวิธีพีทีบีดี (PTBD) ซึ่งเป็นการตรวจทางด้านรังสีร่วมรักษาโดยใช้รังสีแบบต่อเนื่อง (Fluoroscopy) นั้น จะมีความเสี่ยงที่จะได้รับปริมาณรังสีที่ผิวหนังสูงกว่าการตรวจวินิจฉัยอื่นๆ งานวิจัยนี้ทำการศึกษาปริมาณรังสีที่ผิวหนังที่ผู้ป่วยได้รับว่าอยู่ในระดับที่ปลอดภัยหรือไม่

วัตถุประสงค์หลักจากการศึกษานี้คือวัดปริมาณรังสีที่ผิวหนังของผู้ป่วยต่อการตรวจและเพื่อศึกษาปัจจัยที่มีผลต่อปริมาณรังสีที่ผิวหนังของผู้ป่วยได้รับ โดยใช้เครื่องมิคซอฟ (MIDSOF) ที่เป็นซินทิลเลเตอร์และแคปมิเตอร์ (KAP meter) ทำการวัดในผู้ป่วยทั้งหมด 62 ราย ผู้ป่วย 54 รายได้รับการตรวจทีเอซีอีและ 8 รายที่ได้รับการตรวจพีทีบีดี ในหน่วยงานรังสีร่วมรักษา โรงพยาบาลจุฬาลงกรณ์ สภากาชาดไทย ผลการศึกษาการตรวจรักษาด้วยวิธีทีเอซีอี ปริมาณรังสีเฉลี่ยที่ผิวหนังของผู้ป่วยที่วัดด้วยเครื่องมิคซอฟมีค่า 1.71 ± 1.14 (0.023 – 5.48) เกรย์ และผลจากการคำนวณปริมาณรังสีสมมูลย์เฉลี่ยของการตรวจด้วยเครื่องเอกซเรย์ระบบฟลูออโรสโคปี (Fluoroscopy) มีค่า 70.86 (15.57-188.55) มิลลิซีเวิร์ท ปริมาณรังสีสมมูลย์เฉลี่ยของการตรวจด้วยเครื่องเอกซเรย์คอมพิวเตอร์ (CT) มีค่า 6.93 (3.19 - 20.47) มิลลิซีเวิร์ท จากการศึกษาความสัมพันธ์ระหว่างปริมาณรังสีเฉลี่ยที่ผิวหนังของผู้ป่วยที่วัดได้การเครื่องมิคซอฟ จะมีความสัมพันธ์กับค่าที่ได้จากแคปมิเตอร์สูง ที่ค่า r เท่ากับ 0.76 และพบว่าผู้ป่วยจำนวน 12 รายจากการตรวจทีเอซีอีที่ได้รับปริมาณรังสีที่ผิวหนังเกิน 2 เกรย์ อันมีผลให้เกิดผิวหนังเป็นผื่นแดงและผิวหนังลอก ผลการศึกษาการตรวจรักษาทางเดินน้ำดีโดยวิธีพีทีบีดี ปริมาณรังสีเฉลี่ยที่ผิวหนังของผู้ป่วยได้รับ 0.14 ± 0.21 (0.004 - 0.7) เกรย์และผลจากการคำนวณหาปริมาณรังสีสมมูลย์เฉลี่ยมีค่า 5.69 ± 7.01 (0.43– 22.6) มิลลิซีเวิร์ท

ประโยชน์จากการศึกษานี้เป็นการรายงานถึงปริมาณรังสีที่ผิวหนังของผู้ป่วยและปริมาณรังสียังผลเฉลี่ยที่ผู้ป่วยได้รับในการตรวจรักษา เพื่อเป็นการสร้างความตระหนักให้แพทย์และผู้ที่เกี่ยวข้องคำนึงถึงปริมาณรังสีที่ผู้ป่วยได้รับและปัจจัยที่มีผลต่อปริมาณรังสี เพื่อป้องกันอันตรายที่จะก่อให้เกิดอันตรายจากรังสีแก่ผู้ป่วยในการตรวจทีเอซีอี และพีทีบีดี

ภาควิชา รังสีวิทยา

สาขาวิชา ฉายาเวชศาสตร์

ปีการศึกษา 2559

ลายมือชื่อนิติต

ลายมือชื่อ อ.ที่ปรึกษาหลัก

ลายมือชื่อ อ.ที่ปรึกษาร่วม

587407730 : MAJOR MEDICAL IMAGING

KEYWORDS: PATIENT SKIN DOSE / TRANSARTERIAL CHEMOEMBOLIZATION (TACE) / PERCUTANEOUS TRANSHEPATIC BILIARY DRAINAGE (PTBD) / MINIATURE INVISIBLE DOSIMETER USING SCINTILLATOR WITH OPTICAL FIBER (MIDSOF)

SAIWAROON TEANKUAE: Patient Dose Measurement in TACE and PTBD Procedures Using Scintillation with Optical Fiber Dosimeter. ADVISOR: ASSOC. PROF. ANCHALI KRISANACHINDA, Ph.D., CO-ADVISOR: PROF. MASAYORI ISHIKAWA, Ph.D., 97 pp.

The scintillation dosimeter is most suitable for skin dose measurement for its small size of detector, easily use and there was no need to estimate the surface area exposure. However, scintillation detector could identify the result in limited area because of the small size of detector. During the procedure to identify the selected vascular supply tumor, the CT was scanned in patients which increasing the surface dose. TransArterial ChemoEmbolization (TACE) procedure and Percutaneous Transhepatic Biliary Drainage (PTBD) are the procedures producing high dose to both patients and staff. Radiation skin injury to patient was reported by these interventional procedures. The objective of this study is to determine patient skin dose measured by the scintillation detector, MIDSOF.

TACE procedure using Angiographic and CT systems, PTBD procedure using Angiographic system, manufactured by Toshiba Medical System Corporation at Interventional Radiology Unit, King Chulalongkorn Memorial Hospital, the patient skin dose was measured by MIDSOF dosimeter. The patient data, the air kerma area product (KAP) and DLP had been recorded. The equivalent dose was calculated from DLP (mGy.cm) values displayed on CT console and from KAP (Gy.cm²) displayed on fluoroscopic procedures.

TACE procedure included fifty-four consecutive patients (11 female and 43 male) during the period of July 2016 to February 2017. The mean \pm SD of age, height, weight and BMI were 63.3 \pm 9.9 years, 164 \pm 8.4 cm, 65.7 \pm 10.1 kg and 24.4 \pm 3.4 kg/m² respectively. The mean \pm SD of fluoroscopic time, total number of radiographic frames were 33 \pm 15 min and 220 \pm 194 respectively. The mean \pm SD of patient skin dose was 1.71 \pm 1.14 (0.023 – 5.48) Gy. The mean \pm SD of patient dose determined by KAP was 379.88 \pm 147.78 (59.9 – 725.2) Gy.cm². The correlation, r between the air kerma area product, KAP (Gy.cm²) and patient skin dose determined by MIDSOF (Gy) was 0.76. The mean equivalent dose with range of fluoroscopic and CT procedures were 70.86 (15.57-188.55) and 6.93 (3.19 - 20.47) mSv respectively.

PTBD procedure included eight consecutive patients (2 female and 6 male). The mean \pm SD of KAP values were 21.9 \pm 26.9 (1.67 – 87) Gy.cm². The mean \pm SD of the equivalent dose and range was 5.69 \pm 7.01 (0.43–22.6) mSv. The mean \pm SD of patient absorbed dose and range were 0.14 \pm 0.21 (0.004 - 0.7) Gy. In this study, 12 patients from TACE procedure received the skin dose exceed 2 Gv for erythema and epilation at prompt and early exposures.

Department: Radiology
Field of Study: Medical Imaging
Academic Year: 2016

Student's Signature

Advisor's Signature

Co-Advisor's Signature

ACKNOWLEDGEMENTS

I would like to express thankfulness and deepest appreciation to Associate Professor Anchali Krisanachinda, Ph.D., Department of Radiology, Faculty of Medicine, Chulalongkorn University, my advisor for her helpful, suggestion, supervision, guidance, constructive direction and polishing of the thesis writing to improve the English expression.

I would like to thank Professor Franco Milano, University of Florence Italy, who is the external examiner of the thesis defense for his constructive comments, recommendation and teaching of knowledge in Medical Imaging.

I would like to thank Professor Masayori Ishikawa, Ph.D., Faculty of Health Sciences, Hokkaido University, Sapporo, Japan, my teacher for support patient skin dosimeter, MIDSOF, for the research purpose.

I would like to thank Associate Professor Sivalee Suriyapee, Head Physicist at Division of Radiation Oncology, Department of Radiology, Faculty of Medicine, Chulalongkorn University, my teacher for her advice and comments in the research.

I would like to deeply thank Ms. Petcharleeya Suwanpradit, Department of Radiology, King Chulalongkorn Memorial Hospital, for her helpful suggestion and contribution in equipment QC part in this research.

I am thankful for all lecturers and staff at Master of Science Program in Medical Imaging, Faculty of Medicine, Chulalongkorn University for their suggestions and teaching knowledge during the course of Medical Imaging.

I would like to thank all Radiological technologists at Interventional Radiology unit, King Chulalongkorn Memorial Hospital for their kind supports.

Finally, I am greatly thankful to my family for their invaluable encouragement, entirely care, financial support and understanding during the entire course of the study.

CONTENTS

	Page
THAI ABSTRACT	iv
ENGLISH ABSTRACT.....	v
ACKNOWLEDGEMENTS.....	vi
CONTENTS.....	vii
LIST OF TABLES	1
LIST OF FIGURES	2
LIST OF ABBREVIATION	4
CHAPTER I.....	5
INTRODUCTION	5
1.1 Background and rationale.....	5
1.2 Research objective.....	8
CHAPTER II	9
REVIEW OF RELATED LITERATURE.....	9
2.1 Theory	9
2.1.1 Introduction of digital subtraction angiography (DSA) system ..	9
2.1.2 Flat panel detector (FPD) fluoroscopy systems	10
2.1.3 Air kerma area product (KAP)	12
2.1.4 The Computed tomography (CT)	12
2.1.5 Ionizing radiation and patient dose.....	14
2.1.6 Effective dose	15
2.1.7 Transarterial chemoembolization (TACE).....	16
2.1.8 Percutaneous transhepatic biliary drainage (PTBD)	17
2.1.9 Development of ultra miniature invisible dosimeter using scintillator with optical fiber (MIDSOF).....	17
2.2 Review of Related Literature	20
CHAPTER III	24
RESEARCH METHODOLOGY	24
3.1 Research design.....	24

	Page
3.2 Research design model	24
3.3 Conceptual framework	25
3.4 Research question	26
3.5 Sample	26
3.5.1 Target population	26
3.5.2 Sample population	26
3.5.3 Eligible criteria	26
3.5.3.1 Inclusion criteria	26
3.5.3.2 Exclusion criteria	26
3.5.4 Sample size determination	27
3.6 Materials	27
3.6.1 Research Equipment	27
3.6.2 Quality control materials	28
3.6.3 Miniature invisible dosimeter using scintillator with optical fiber (MIDSOF)	32
3.6.4 The patients	32
3.6.5 Data recording, complexity index and case consent forms	32
3.7 Methods	32
3.7.1. Perform QC in digital Flat-panel Radiographic –Fluoroscopic system	32
3.7.2 Perform the quality control of CT	32
3.7.3 Calibrate Miniature Invisible Dosimeter using Scintillator with Optical Fiber (MIDSOF) with calibrated ion chamber	33
3.7.4. Data Collection	33
3.7.5. Dosimetric procedure	33
3.7.6 Record patient doses from MIDSOF and KAP	33
3.7.7 Study the relationship between cumulative skin dose and exposure parameters	33
3.7.8 Effective dose calculation	33
3.8 Variables measurement	34

	Page
3.9 Statistical analysis	34
3.10 Data analysis.....	34
3.11 Outcomes	34
3.12 Expected benefits	35
3.13 Limitation	35
3.14 Ethical consideration	35
CHAPTER IV	36
RESULT	36
4.1 Quality control of the DSA equipment.....	36
4.2 Quality control of the CT scanner	36
4.3 The transarterial chemoembolization (TACE) procedures patient studies.....	36
4.4 Average values of technical parameters.....	39
4.5 Procedure performed with a Flat-panel system.....	40
4.6 The total air kerma product ($Gycm^2$) and patient skin dose determined by MIDSOF (Gy) of TACE procedure.....	43
4.7 The effective dose was determined by KAP method	45
4.8 The Complexity index	48
4.9 The correlation between the dose air kerma product, KAP ($Gycm^2$) and patient skin dose determined by MIDSOF (Gy) of TACE procedure.....	48
4.10 The relation between patient skin dose determined by MIDSOF (Gy) and the affecting factor in TACE procedure.	49
4.11 The percutaneous transhepatic biliary drainage (PTBD) patient studies.....	51
4.12 The relation between patient skin dose determined by MIDSOF (Gy) and the affecting factor in PTBD procedures.	52
CHAPTER V	55
DISCUSSION AND CONCLUSION	55
5.1 Discussion	55

	Page
5.1.1. The patients	55
5.1.2. Comparison of the result with other studies	57
5.1.3. Factors affecting radiation dose.....	58
5.1.4 The patient skin dose determined by MIDSOF and System FPD	60
5.1.5 The relationship between KAP method and MIDSOF.....	60
5.1.6 The relationship between dose from MIDSOF and dose from monitor.....	61
5.1.7 The effective dose	61
5.2 Conclusion.....	62
REFERENCES	64
APPENDIX.....	66
APPENDIX A.....	67
Case Record Form	67
APPENDIX B.....	71
Patient Information Sheet.....	71
APPENDIX C.....	78
Consent form	78
APPENDIX D.....	80
Complexity Index	80
APPENDIX E	86
Equipment performance for DSA system	86
Equipment performance for CT system	89
VITA.....	97

LIST OF TABLES

Table	Page
1. 1 Various dosimeters with their problems in clinical use.....	8
3. 1 Radcal Accu-gold Digitizer module.....	30
4. 1 The 54 patient data underwent TACE procedure.....	37
4. 2 The summary of patient data underwent TACE procedure.	39
4. 3 Mean values of technical parameters.....	39
4. 4 The patient data performed with a digital flat-panel system in TACE procedure.....	40
4. 5 The factors affecting patient dose in TACE procedure.	42
4. 6 The total dose air kerma product ($Gycm^2$) and patient skin dose determined by MIDSOF (Gy) and system detector on TACE procedure.	43
4. 7 The effective dose determined by KAP method and the effective dose determined by DLP in TACE procedure.....	46
4. 8 The patient data underwent PTBD procedure from 8 patients.	52
5. 1 The patients who received the skin dose exceed the transient erythema.....	55
5. 2 Tissue reaction from single-delivery radiation dose to skin.....	56
5. 3 Five bands of patient skin dose measured by MIDSOF and by system detector (Gy).....	57
5. 4 Comparison of KAP readouts with other studies during TACE procedure....	57

LIST OF FIGURES

Figure	Page
2. 1 Subtraction images.....	10
2. 2 Construction of an FPD array.	11
2. 3 Images from Transarterial Chemoembolization (TACE) procedures.....	16
2. 4 Transarterial chemoembolization (TACE) procedure.	17
2. 5 Percutaneous transhepatic biliary drainage (PTBD).....	17
2. 6 Energy dependency at tube voltage	18
2. 7 Dose rate (mGy/min) dependency	19
2. 8 Angular dependency	19
2. 9 Schematic diagram of SOF dosimeter system	20
2. 10 Three dosimeters dedicated for skin dose	21
2. 11 SOF probe is invisible on fluoroscopic image in comparison to SDM & PSD	21
2. 12 The entrance surface dose determined by Unfors PSD methods in.....	22
2. 13 Maximum entrance surface dose, ESD on left, middle and right lobes.....	22
2. 14 Maximum skin dose, cGy from neurointervention, PTBD.....	23
3. 1 Toshiba IVR-CT.....	27
3. 2 KAP meter installed on collimator of the X-ray tube.	28
3. 3 Cylindrical PMMA phantom of 16 cm diameter.	28
3. 4 Copper sheets.	29
3. 5 The 10X6-3CT Detector 10 cm length of the pencil-type ionization.	29
3. 6 The AGMS-D+ is a Solid State.	30
3. 7 CIRS Model 903 phantom	31
3. 8 Catphan Phantom.....	31
3. 9 MIDSOF and display system	32
3. 10 MIDSOF placed on patient's back at a point over the liver	33

LIST OF FIGURES

Figure	Page
4. 1 The effective dose in TACE patients using fluoroscope and CT procedures .	48
4. 2 The correlation between the dose air kerma product, KAP (Gycm ²) and patient skin dose determined by MIDSOF (Gy)	49
4. 3 The relation between the patient skin dose determined by MIDSOF (Gy) and the fluoroscopic time in second.....	49
4. 4 The relation between the patient skin dose determined by MIDSOF (Gy) and total number of radiographic frames.	50
4. 5 The relation between the patient skin dose determined by MIDSOF (Gy) and the patient BMI (kg/m ²).	50
4. 6 The relation between the patient skin dose determined by MIDSOF (Gy) and the experience of interventional radiologists.....	51
4. 7 The correlation between the dose air kerma product, KAP (Gycm ²) and patient dose (mGy) from 8 cases in PTBD procedure	52
4. 8 The relation between the patient skin dose (mGy) and the fluoroscopic time in second.....	53
4. 9 The relation between the patient skin dose (mGy) and total number of frames.	53
4. 10 The effective dose underwent PTBD procedure from 8 patients.....	54

LIST OF ABBREVIATION

AK	Air Kerma
ESD	Entrance Skin Dose
FDA	Food and Drug Administration
FOV	Field of view
Gy	Gray
HVL	Half-Value Layer
KAP	Air kerma area product
kVp	Kilovoltage peak
mAs	Milliamperere second
mGy	milliGray
QA	Quality Assurance
QC	Quality Control
r	Correlation coefficient
s	Second
SD	Standard Deviation
SID	Source to Image Distance
Sv	Sievert

CHAPTER I

INTRODUCTION

1.1 Background and rationale

Interventional radiology has been an essential part of modern patient treatment using fluoroscopically guided interventional radiological procedure for more than 10 years. Radiation-induced skin injury has also been increasingly reported in the literature and received growing attention among the medical community. Therefore; it is important to estimate the patient skin dose and try to reduce it.

Interventional radiology involves in the treatment of various diseases for several decades. Transarterial chemoembolization (TACE) has been used extensively in non-operative treatment of hepatocellular carcinoma (HCC) patient. TACE has a role in delaying the progression of HCC unit when a donor liver becomes available. TACE is an interventional radiology procedure, involves percutaneous access to the hepatic artery usually by puncturing the common femoral artery at the right groin and passing a catheter through the abdominal aorta, through the celiac axis and common hepatic artery, into the feeding arteries supplying the tumors. Chemotherapeutic dose is directed to the tumor following embolization for ischemic effect of the tumors. TACE is the high exposure procedure for both patients and staff in routine clinical service at King Chulalongkorn Memorial Hospital (KCMH). Radiation skin injuries to patient can be caused by this interventional procedure. Therefore, the avoidance of skin injuries during the procedure is needed.

Two types of radiation effect may occur are deterministic and stochastic effects.

1. Deterministic effects

Based on a large number of experiments involving animals and other researches, further supplemented by theoretical studies, it was discovered that severity of certain effect on human being would increase with increasing dose. There exists a certain level, the threshold, below which the effect is not observed. This kind of effect is called deterministic effects such as cataract, erythema, infertility etc.

The characteristics of deterministic effects are shown as the followings:

1. Damage depends on absorbed dose.
2. The existence of the threshold dose.

2. Stochastic effects

The severity of stochastic effects does not depend on the absorbed dose. Under certain exposure conditions, the effects may or may not occur. There is no threshold and the probability of having the effect is proportional to the dose absorbed such as radiation induced cancer and genetic effects.

The characteristics of stochastic effects are shown as the followings:

1. Severity is independent of absorbed dose.
2. The non - existence of the threshold dose.
3. The probability of occurrence depends on absorbed dose. [1]

Angiography is a medical imaging technique used to visualize the blood vessels and organs of the body, with particular interest in the arteries, veins, and the heart chambers. This is traditionally done by injecting a contrast agent into the blood vessel and imaging using X-ray fluoroscopy based techniques. Digital Subtraction Angiography (DSA) is type of fluoroscopic technique to clearly visualize blood vessels and has been the “gold standard” for many vascular and cerebrovascular imaging studies. Images are produced using contrast media by subtracting pre-contrast image (mask) from contrast images. [2]

Computed tomography (CT) is a method which X-rays and computers produce the medical images for analyses. Beams of x-rays pass from tube through patient's body at different angles to the detectors, and then the images are reconstructed by the computer software. CT Angiography (CTA) is a combined CT scan with injection of contrast media through the venous vessel produce image of blood vessels and tissues. [2]

The most convenient and widely used method for indirect radiation dose monitoring in DSA is the air kerma area product (KAP) meter. The KAP measurements using a flat x-ray transmission ionization chamber have been accepted as a suitable dosimetric technique for angiographic examination. KAP measurements are commonly used to assess the effective dose for evaluation of stochastic risk. Modern devices design for the simultaneous measurement of KAP and air kerma diagnostic radiology during fluoroscopy and exposure. KAP has the advantage of being constant at any distance from the tube focus, so wherever KAP is measured; it reflects the air kerma radiation field size at the patient's skin. The KAP is also useful in estimating the effective dose via calculation of the total energy imparted to the patient, which can be used to calculate the stochastic risk. [3]

Requirement of Individual dosimeter for patients

Recently, monitoring of skin dose is desired at clinical sites to reduce skin injuries by excessive x-ray exposure during the interventional radiology (IR) procedures. International Commission on Radiation Protection, ICRP recommended that the absorbed dose excess of 1 Gy in patient must be recorded. There are several types of dosimeter to monitor the patient dose but there are limitations in using those dosimeters such as the conventional ionization chamber for diagnostic x-rays. The detector size is not small enough due to less efficiency. Semiconductor dosimeter is not suitable for fluoroscopy because it has metal cable, clearly displayed on fluoroscopy image.

Journal of Radiation Research reported on development of ultra miniature invisible dosimeter using scintillator with optical fiber for diagnostic X-ray dosimetry (MIDSOF dosimeter)[4]. MIDSOF dosimeter is commercially available skin dosimeters. The new SOF dosimeter dedicated for diagnostic X-ray dosimeter is not only invisible on fluoroscopic image, but also having good properties concerning to dose dependency, dose rate dependency and energy dependency. [4]

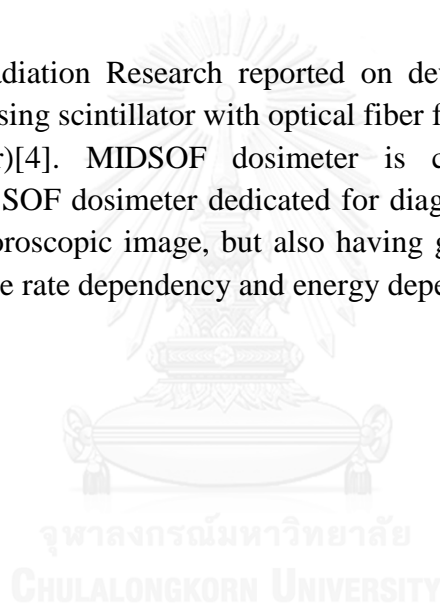


Table 1. 1 Various dosimeters with their problems in clinical use.

Dosimeters	Problems in clinical use
Skin dose monitor (SDM)	<ul style="list-style-type: none"> ▪ Cadmium used in probe
Shadow Free chamber (SFC) Patient Skin Dosimeter (PSD)	<ul style="list-style-type: none"> ▪ Detector or metal cables are clearly appeared on fluoroscopy image.
Area dosimeter	<ul style="list-style-type: none"> ▪ Accumulating entire area dose during treatment. ▪ Difficult to monitor skin dose for specific area.
Thermoluminescent dosimeter (TLD) Optically stimulated luminescence(OSL) Radiographic dosimeter	<ul style="list-style-type: none"> ▪ Post -operation required, not real-time monitoring. ▪ Difficult to prevent overdose to the skin.
Radiochromic dosimeter	<ul style="list-style-type: none"> ▪ Color changes indicate accumulated dose. ▪ Difficult to monitor the color change at under-tube condition.

1.2 Research objective

1. To determine the patient radiation dose from TACE and PTBD procedures using SOF dosimeter.

2. To identify parameters influence the patient skin dose in TACE and PTBD procedures.

CHAPTER II

REVIEW OF RELATED LITERATURE

2.1 Theory

2.1.1 Introduction of digital subtraction angiography (DSA) system [5]

Diagnostic cerebral and peripheral angiography utilizes modified techniques that are extensions of those used in the coronary arterial system. Visualization of a vascular bed is made possible under fluoroscopy by injecting radio opaque contrast into the proximal vessel. These images allow two dimensional visual assessment if orthogonal views are taken. Characteristics of contrast flow through a vessel and pressure measurements allow acquisition of hemodynamic data that represent functional competence of an artery. DSA has become an imaging standard for evaluation of vascular anatomy. First introduced in 1970s, it is highly effective in contrasting arterial structures with their surrounding bone and soft tissue. DSA was firstly used in humans in 1978 and was made commercially available in 1980.

Digital fluoroscopy [6]

Digital fluoroscopy is most commonly configured as a conventional fluoroscopy system (tube, table, image intensifier, video system) in which the analog video signal has been digitized with an Analog to Digital Converter (ADC). Alternatively, digitization may be accomplished with a digital video camera (such as a charge-coupled device) or via direct capture of x-rays with a flat panel detector. For digital fluoroscopy system in which the analog video signal is digitized with an ADC, the resolution is limited by the resolution of the video camera, which is typically 1–2 line pairs per millimeter.

For the typical system, the ADC samples the analog video signal at discrete time points and converts the value of the signal to a binary number for storage. The maximum and minimum analog video signal values will be scaled to the maximum and minimum digital values according to the bit depth of the ADC. An 8-bit ADC will convert the video signal to a maximum of 256 different values. Improved representation of the analog video signal will occur as the bit depth of the ADC is increased and the sampling frequency of the discrete time points increases.

The digital image data from digital fluoroscopy may be processed by using many useful image processing techniques. These techniques may serve to decrease radiation exposure to the patient and medical imaging staff or improve visualization of anatomy. Processing options include last image hold, gray-scale processing, temporal frame averaging, and edge enhancement. Additional processing is available when digital fluoroscopy data are used to perform DSA.

DSA acquisition [6]

The acquisition of digital fluoroscopic images can be combined with injection of contrast material and real-time subtraction of pre and post-contrast images to perform examinations that are generally referred to as digital subtraction angiography (Figure 2.1).

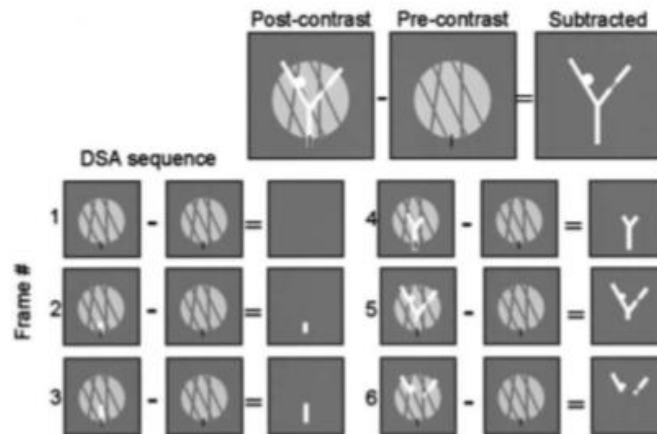


Figure 2. 1 Subtraction images.

A pre-contrast mask image (showing a distracting background structure and the tip of a catheter,) is subtracted from a post-contrast image obtained at the same location (showing contrast material–filled vessels). The result is an image of only the contrast material–filled vessels. During the actual imaging sequence, the subtraction process may begin slightly prior to contrast material injection, with each frame capturing a different phase of the injection. The sequence of subtracted frames can then be reviewed in cine mode or as still frames. The unsubtracted original digital fluoroscopic images are generally not reviewed.

2.1.2 Flat panel detector (FPD) fluoroscopy systems [6]

FPD fluoroscopy systems have begun to dominate angiography and cardiac catheterization laboratory. The smaller size of the FPD imaging chain allows for more flexible movement during patient examinations. Moreover, FPD systems do not require a television camera to produce an electronic signal for the display monitor.

FPD produces a digital electronic signal, which represents the intensity of the x-rays that impinge on each detector element (DEL) in the solid-state FPD array. Moreover, the entire process is digital, which reduces image noise caused by electronic components.

The FPD consists of an array of individual DELs (Figure 2.2a). The typical size of those in fluoroscopy systems ranges from 140 μm to about 220 μm per side, depending on the manufacturer and model. The size of the entire array ranges from 25 \times 25 cm^2 to 40 \times 40 cm^2 . However, some manufacturers specify the size of the FPD by providing a diagonal measurement, and others quote the edge dimension. A FPD may contain 1.5–5.0 million individual DELs to make a uniform array of DELs.

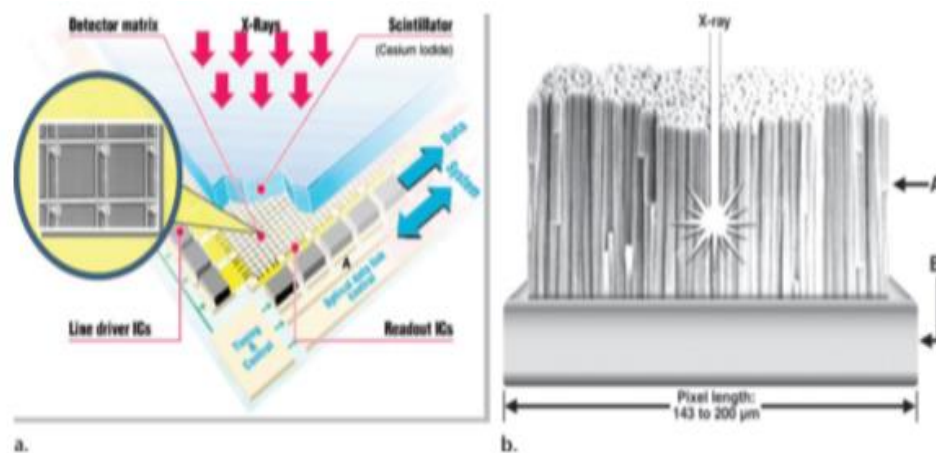


Figure 2. 2 Construction of an FPD array. (a) Drawing shows a section of the FPD and many individual DELs. A - 14-bit A/Ds, IC - integrated circuit. (b) Drawing shows one DEL in the FPD array. A - CsI needle scintillator layer, B - photodiode and transistor layer.

Currently, most FPD arrays are indirect solid-state systems, meaning that the x-ray energy is firstly converted to light and then to an electronic signal. An individual DEL consists of a scintillation layer, which composes of thallium-activated CsI (Figure 2.2b). The scintillation layer attenuates the incident x-rays and produces light. The CsI scintillation layer is composed of many needle-like crystals, which are grouped together to cover the surface of the DEL. These needle-like structures help direct light toward the photodiode located below. The amount of light produced is directly related to the amount of x-ray flux that is incident on the DEL. When light hits the surface of the low noise photodiode and transistor below, it acts like a switch, allowing the diode to conduct electricity. In the absence of light on its surface, the photodiode acts like an insulator, preventing the flow of electrons.

Each DEL is able to quantify the amount of x-ray radiation incident upon its surface. First, an electronic switch is closed and the capacitor is charged. Next, the electronic switch is opened. Because no light is incident upon the surface of the DEL, the charge remains on the capacitor, which stores the initial charge, similar to the way bank stores money. The interaction of x-rays with the scintillator produces light in

proportion to the x-ray flux. This light causes the photodiode to conduct to different degrees, depending on the intensity of the light. As more light is produced, more charge is drained from the capacitor, like a bank withdrawal of money. Finally, another electronic switch is closed and the remnant charge is withdrawn from the storage capacitor and sent to the display system. The loss in charge is related to the amount of x-ray radiation incident upon the DEL. By reading each DEL in the FPD array row by row, an electronic image of the distribution of x-rays that are incident upon the FPD can be formed. In this way, an FPD array is used to create an image without the use of a television camera.

2.1.3 Air kerma area product (KAP) [7]

Air kerma area product (KAP) is defined as the air KERMA multiplied by the area of the X-ray beam in the plane perpendicular to the beam axis. It is usually measured in $\text{Gy}\cdot\text{cm}^2$ and radiation back-scattered from the patient is excluded. Provided that the cross sectional area of the beam lies completely with the detector, it may be shown by simple application of the inverse square law that the reading will not vary with the distance from the tube focus. Thus the KAP can measure at any point between the diaphragm housing on the X-ray tube and the patient, but not so close to the patient that there is significant backscattered radiation.

KAP meters consist of flat, large area parallel plate ionization chambers connected to suitable electrometers which respond to the total charge collected over the whole area of the chamber. The meter is mounted close to the tube focus where the area of the X-ray beam is relatively small and dose rates are high. It is normally mounted on the diaphragm housing where it does not interfere with the examination and is usually transparent so that when fitted to an over-couch X-ray tube the light beam diaphragm device can still be used.

KAP measures of total energy fluence incident on the patient and related to the energy absorbed in the patient. Some studies for which KAP meters should be used include barium enemas, barium meals, micturatingcystograms, cardiac investigations and interventional techniques in neuroradiology and biliary procedures.

2.1.4 The Computed tomography (CT) [8]

CT is an imaging technique that produces cross-sectional images, representing in each pixel the local X-ray attenuation properties of the body. The first experimental set-up of Hounsfield in 1970 worked with the translation/rotation principle. A thin beam of X-rays was generated through the use of a collimator and a single detector element to measure the attenuated intensity. By translating this set-up, different positions were

measured. After an entire set of parallel measurements had been acquired, the set-up was rotated to acquire the next parallel projection. This principle is the first generation of CT scanner.

The second generation of CT scanners differed only slightly from that initial design in that a small number of measurement values could be obtained simultaneously. In Hounsfield's first scanner a total of 180 projections were obtained in steps of 1° with 160 measurement values each. The acquisition of those 28,800 measurement values took five minutes. From that data an image of 80×80 pixels was reconstructed. With such a scanner, a head examination requiring six slices took about half an hour. Therefore, physicists were aiming at shortening the acquisition time. This was achieved with the introduction of the third generation CT scanners: a 1D array of detector elements positioned on an arc covers the entire measurement field and acquires a complete 'fan-beam' projection. This not only avoided the slow translation movements, but also improved the efficiency of using the output of the X-ray tube.

The third generation CT scanner consisted of a donut-shaped gantry with a big bore. Head, body, arms or legs were in the middle of the gantry to make a cross-sectional image. The patient is moved in and out on a motor-controlled table. The slice thickness is usually 0.5 to several mm and the spatial resolution, in the cross section, is roughly 1 mm at 512×512 pixels per slice.

Within the gantry of the CT scanner, an X-ray tube is placed opposite a detector array with up to 1200 detecting elements receiving the photons that passing through the patient. If one measurement has been done this way, the source and detector rotate over a small angle (roughly 1°) and a new measurement is taken. The scanner repeats this procedure until a rotation of 180° has been reached. Then all thousands of measurements for reconstructing one slice have been done. The table on which the patient lies can then move a little further through the gantry for measuring a new slice.

Fourth generation followed with stationary detectors fully encircling the patient so that only the x-ray tube rotated. Rotatory systems were quickly accepted, and translation-rotation systems meanwhile disappeared completely. The third generation has prevailed and constitutes the standard approach in clinical scanners today.

Computed tomography angiography (CTA) definition [9]

CTA is a combined CT scan with injection of contrast media through the venous vessel in arm to produce image of blood vessels and tissues. CTA is primarily performed for assessing the heart, arteries, or veins. It requires at a minimum a thin section helical (spiral) CT acquisition coupled with a power injection of intravenous iodinated contrast medium. Three-dimensional rendering and multi-planar reformations (MPR) are important components of many CTA examinations.

2.1.5 Ionizing radiation and patient dose [9]

Doses from CT examinations are generally significantly higher than those from conventional X-rays, although a CT scan provides more diagnostic information. Recent UK surveys reported conventional X-ray examinations with average doses of 0.04 mSv for head examinations, 0.02 mSv for chest and 0.7 mSv for abdomen examinations. A similar survey for CT examinations gave values of 1.5, 5, and 6 mSv respectively for the head, chest and abdomen regions. These figures represent average values from the use of a wide range of operational parameters, such as tube current and voltage, however they can be used as a guide.

The standard reference parameters used to describe dose in CT are the volume computed tomography dose index (CTDI_{vol}) and the dose length product (DLP). The CTDI_{vol} is calculated from measurements, made with a 100 mm long pencil ion chamber, in standard sized polymethyl methacrylate (PMMA) head and body phantoms which have been irradiated at the halfway position, along the length, with a single beam rotation. However, as a dose descriptor, it is important to think of the CTDI_{vol} as representing the average dose in a slice of tissue, halfway along a 100 mm irradiated length.

The DLP represents the total amount of irradiation given, and as such gives an indicator of risk (without taking into account the radiosensitivity of particular organs). The CTDI_{vol} is a very useful dose descriptor for comparing dose from different protocols or different scanners. However, comparisons should only be done for scans undertaken on standard size patients. The CTDI_{vol} and DLP values are displayed on the scanner console. It is always invaluable to look at these figures when reviewing patient images for an assessment of the image quality and dose performance of a scanner. Both the CTDI_{vol} and the DLP are used when comparing with dose reference levels (DRLs). Multiple detector computed tomography or (MDCT) scanners have the potential to give higher radiation doses compared to single slice scanners. Their flexibility in scanning lengths with high mAs values, and the ease with which they perform dual and even triple-phase contrast studies, can lead to high patient doses. In addition, there are some intrinsic features of current MDCT design which can give rise to slightly higher doses.

2.1.6 Effective dose [10]

The concept behind effective dose and its predecessor, effective dose equivalent, was proposed in 1975. The aim was to define a quantity that could be related to the probability of health detriment due to stochastic effects from exposure to low doses of ionizing radiation. Effective dose is a sum of the equivalent doses in tissues and organs of the body that are considered to be sensitive to radiation damage, weighted according to the risk of aggregated.

Health detriment. The weighting factors that are used for individual tissues are based predominantly on a statistical analysis of the increase in the long-term incidence and mortality for cancer determined from a life span study (LSS) of the survivors exposed to radiation when the atomic bombs were exploded over Japan, although account is taken of data from other groups of workers and patients who have received high radiation exposures, and of the possibility of hereditary effects.

The application of effective dose in its present form was recommended by the International Commission on Radiological Protection (ICRP) which stated that it was intended for use in radiation protection, including the assessment of risks in general terms. However, effective dose has been applied extensively to medical exposures, often to specific individuals of known gender and age. Effective dose can be used in both the generic justification and the optimization of medical exposures, but should not be used to predict absolute risk levels. Values have been derived for a variety of diagnostic procedures in radiology and nuclear medicine in order to provide a relative index of harm that can be considered in justification of medical exposures.

For medical exposures, conversion coefficients have been derived that allow values for effective dose to be calculated from measurable dose quantities, such as entrance surface dose (ESD) or KAP for radiology examinations and administered activity for nuclear medicine procedures.

Effective dose conversion coefficients

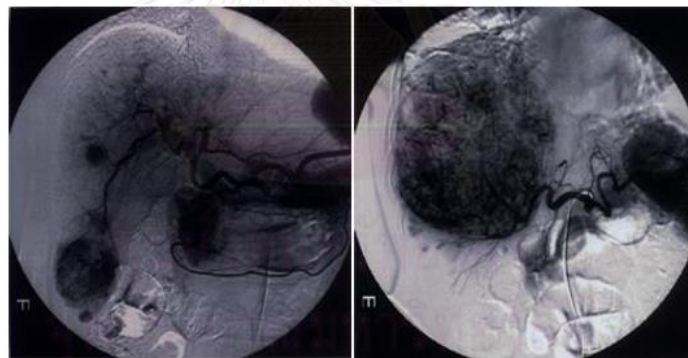
The coefficients have been established from computer simulations for the exposure of anthropomorphic phantoms. The coefficients are quoted to two or three significant figures, but the uncertainties in these and in the tissue weighting factors are seldom considered. The conversion coefficients are derived from mathematical phantoms, which represent idealized anatomical forms in terms of size, shape and position of each tissue. Coefficients used currently for the assessment of effective dose have been based on a variety of models with differences in the positions and sizes of the tissues, although the geometry for a standard human body anthropomorphic phantom has now been specified, on which future computational phantoms should be based.

2.1.7 Transarterial chemoembolization (TACE) [11]

Transarterial chemoembolization (TACE) has been used extensively in the palliative treatment of unresectable hepatocellular carcinoma (HCC), one of the most common malignancies worldwide.

The most common causes are alcoholic and viral hepatitis (C). The standard treatment for HCC is surgical resection, which has a 60% 5 year survival. In case of unresectable tumor or marginal liver function, the current treatment of choice is orthotopic liver transplantation. Due to the scarcity of organ donors and to the multiple carcinomas these patients have, many die while on the transplant list. TACE has a role in delaying the progression of HCC until a donor liver becomes available.

The lifespan for a patient with unresectable HCC could reasonably be extended for 1-2 years with continuing TACE (through the exact benefit would depend heavily on the patient's medical condition)



A พาลงกรณ์มหาวิทยาลัย

B

Figure 2. 3 Images from Transarterial Chemoembolization (TACE) procedures, (A)Multi nodular tumors stain in right hepatic lobe of the patient in TACE procedure, (B)The patient with large HCC supplied by multiple extrahepatic collaterals and accessory left gastric and hepatic calciform arteries from the left hepatic artery.

TACE is an interventional radiology procedure involves gaining percutaneous access to the hepatic artery, usually by puncturing the common femoral artery in the right groin and passing a catheter through the abdominal aorta, (which supplies the liver). The interventional radiologist performs an arteriogram to identify the branches of the hepatic artery supplying the tumors and threads smaller catheters into these branches. This is done to maximize the amount of the chemotherapeutic dose directed to the tumor (Figure 2.3). When a blood vessel supplying tumor has been selected, alternating aliquots of the chemotherapy dose and of embolic particles are injected

through the catheter. The total chemotherapeutic dose may be given in one vessel distribution, or it may be divided among several vessels supplying the tumors.

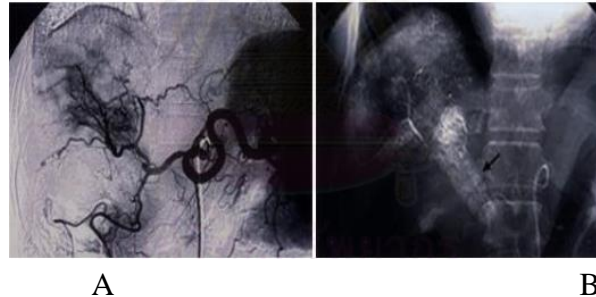


Figure 2. 4 Transarterial chemoembolization (TACE) procedure, (A) The smaller catheters into these branches the hepatic artery supplying the tumor, (B) Simple radiography taken after chemoembolization shows satisfactory lipiodol retention in the main portal tumor thrombi (arrow).

2.1.8 Percutaneous transhepatic biliary drainage (PTBD)

Percutaneous transhepatic biliary drainage is performed in patients with obstruction jaundice in whom endoscopic drainage is unsuccessful or who have complex hilar lesions show in figure 2.5. The commonest indication is in malignant disease of bile duct or pancreas.



Figure 2. 5 Percutaneous transhepatic biliary drainage (PTBD)

2.1.9 Development of ultra miniature invisible dosimeter using scintillator with optical fiber (MIDSOF) for diagnostic X-ray dosimetry. [4]

A novel plastic scintillator based dosimeter (“SOF dosimeter”) had been developed which probe is composed only organic material, tissue equivalent and its physical density is about 1 g/cm^3 , thus the probe cannot be recognized in fluoroscopic image. SOF probe applied optical fiber is flexible and higher efficiency than ionization chamber and adequate for skin dosimetry during IR. However, original SOF probe is dedicated for Ir-192 brachytherapy, not a small energy dependency. SOF dosimeter for brachytherapy applies ordinary organic scintillator because photon production is

proportional to absorbed dose. However, the photon production is not proportional to absorbed dose for diagnostic X-ray, SOF probe, a monomer - based scintillator which has less energy dependency for diagnostic X-ray of tube voltage from 40 to 60 kV than organic scintillator to achieve better energy dependency.

The energy dependency of SOF probe is improved by mixing monomer-based scintillator and Zn_2SiO_4 scintillator.

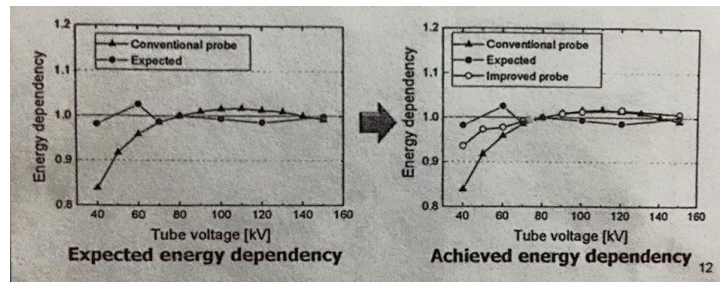


Figure 2. 6 Energy dependency at tube voltage from 40-160 for conventional and improved probes

Energy dependency

The energy dependency of conventional probe normalized at 80 kV varies from (40 kV) at 0.82 to 1.02 at (110 kV).

By mixing the two different scintillators, sensitivity at lower energy was recovered, then the energy dependency of improved probe was achieved ranging from 0.93 at (40 kV) to 1.02 at (120 kV). Moreover, the energy dependency from 50 to 150 kV was with $\pm 3\%$, acceptably small energy dependency was achieved.

Improved SOF probe has the smallest energy dependency among other commercial skin dosimeters. (Figure 2.6)

Dose and dose rate dependency

Good dose linearity ranging from 4 to 2,800 mGy and no limit to maximum dose under adequate dose rate condition because it is counting-type detector.

Good dose rate linearity ranging from 5 to 1,700 mGy/min was reported, however, fluctuation was observed at over 1,200 mGy/min. (Figure 2.7)

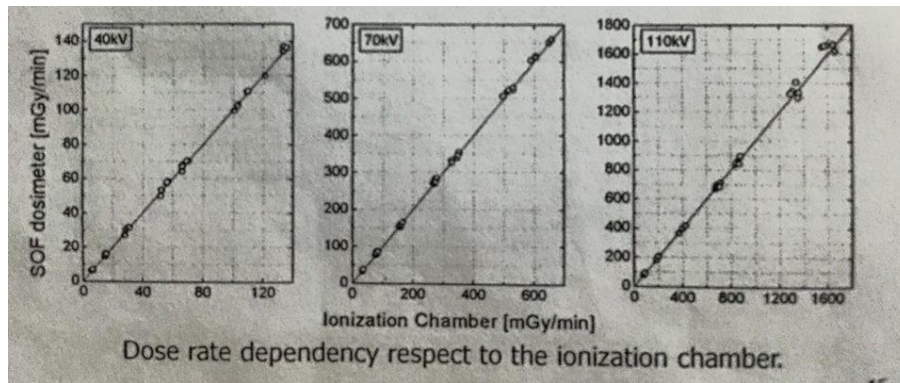


Figure 2. 7 Dose rate (mGy/min) dependency at 40, 70 and 110 kV between SOF dosimeter and ionization chamber

Angular dependency

The very small radial angular dependency was confirmed. It seem to be reasonable because the structure of probe is identical to X-ray incidence.

Low sensitivities at ≤ 40 deg and ≥ 140 deg were caused by decreasing back scattered X-rays (Figure 2.8).

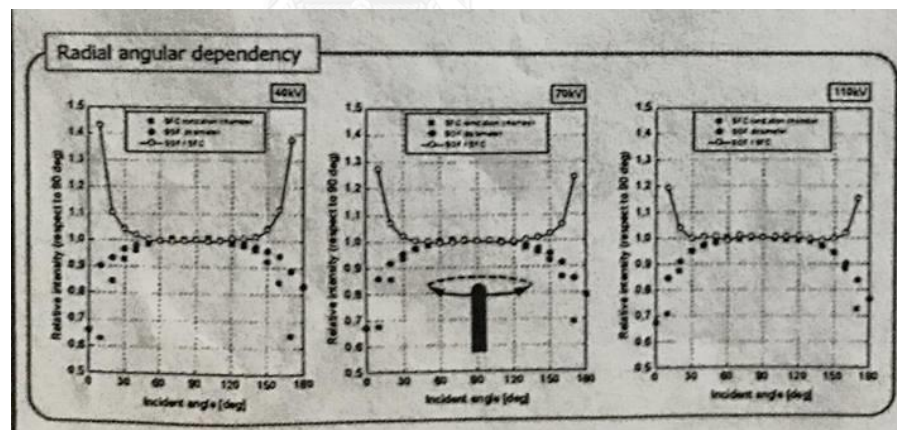


Figure 2. 8 Angular dependency

For the axial angular dependency, the lowest sensitivity was observed at perpendicular irradiation, not a small angular dependency was observed.

The new SOF dosimeter dedicated for diagnostic X-ray dosimetry is not only invisible in fluoroscopic image, but also having good properties concerning to dose dependency, dose rate dependency and energy dependency.

Although the very small radial angular dependency was confirmed, not a small axial angular dependency was observed.

Combination of two different scintillators made the energy dependency much smaller. Further improvement of energy dependency can be expected by mixing additional scintillators.

Since the improved SOF probe has the smallest energy dependency among commercial skin dosimeters and transparent to diagnostic X-ray, The SOF dosimeter will contribute not only for skin dosimetry but also quality assurance of X-ray devices.

2.2 Review of Related Literature

Ishikawa, M. [4] reported in Journal of Radiation Research on Development of ultra miniature invisible dosimeter using scintillator with optical fiber for diagnostic X-ray dosimetry (MIDSOF dosimeter). They have developed a novel plastic scintillator based dosimeter which probe is composed only organic material or skin dosimetry.

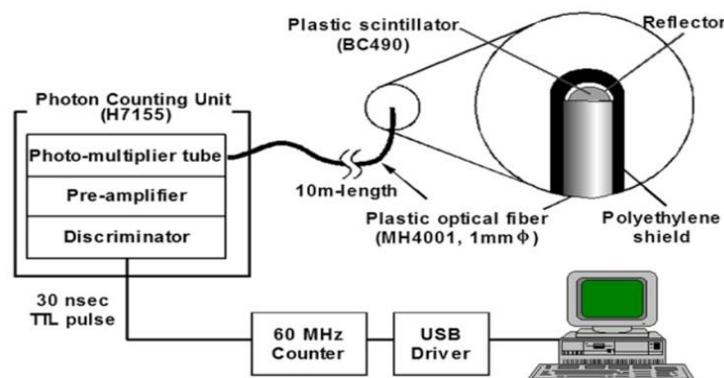


Figure 2. 9 Schematic diagram of SOF dosimeter system

The SOF dosimeter is made up of a small plastic scintillator, a plastic optical fiber, a photon counting unit and data acquisition system connected to a personal computer via Universal serial bus (USB).

Three skin dosimeters

1. Skin dose monitor (SDM) Model 104-101, McMahon Medical (Fig 2.10A)
2. Patient skin dosimeter (PSD), Unfors RaySafe (Fig 2.10B)
3. Miniature invisible dosimeter using scintillator with optical fiber (MIDSOF), Acrobio (Fig 2.10C)



A:SDM

B:PSD

C:MIDSOF

Figure 2. 10 Three dosimeters dedicated for skin dose

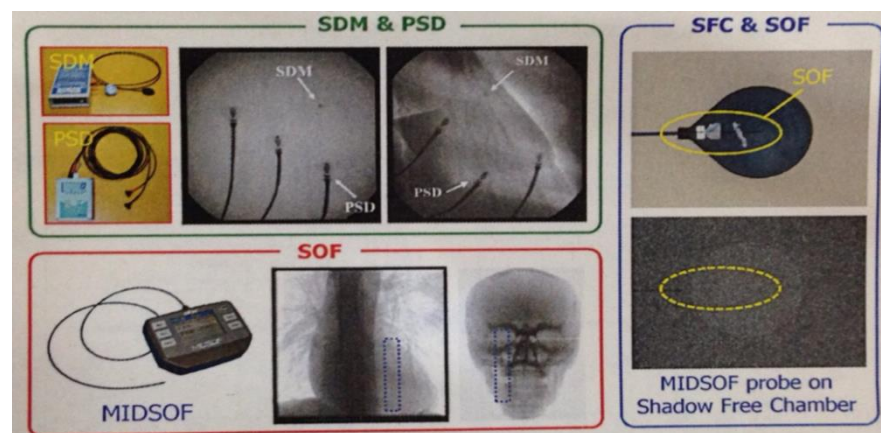


Figure 2. 11 SOF probe is invisible on fluoroscopic image in comparison to SDM & PSD

The new SOF dosimeter dedicated for diagnostic X-ray dosimeter is not only invisible on fluoroscopic image, but also having good properties concerning to dose dependency, dose rate dependency and energy dependency

Although the very small radial angular dependency was confirmed, the axial angular dependency is smaller than 20%. However, MIDSOF probe has acceptable efficiency for wide angle compared to PSD probe.

Combination of two different scintillators made the energy dependency much smaller.

The improved SOF probe has the smallest energy dependency among commercial skin dosimeters and transparent to diagnostic X-ray, the SOF dosimeter will contribute not only for skin dosimetry but also quality assurance of X-ray devices.

Sitthiphan, P. [11] studied the determination of patient effective dose in transarterial oily chemo embolization (TOCE) procedure using digital flat-panel system.

The system is equipped with the air kerma area product (KAP) and used to determine the average entrance surface dose for each procedure. The peak ESD were evaluated by the solid state dosimeter ; Unfors Patient skin dosimeter (PSD) placed on patient back at three regions at left, middle and right portion of liver.

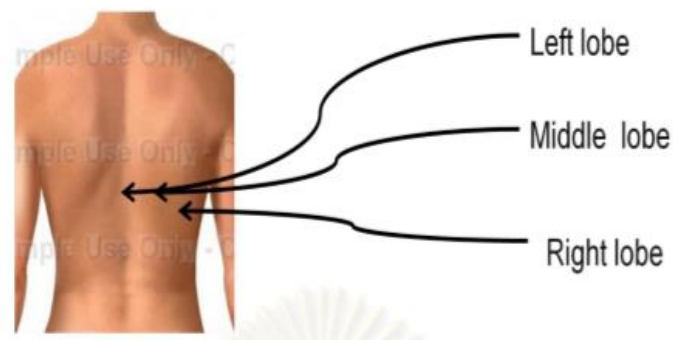


Figure 2. 12 The entrance surface dose is determined by Unfors PSD methods in TOCE procedures.

The entrance surface dose determined by Unfors PSD methods in TOCE procedures.

The average of peak ESD determined by Unfors PSD was 968.66 mGy at left lobe of liver, the middle lobe was 848.41 mGy and the right lobe of liver was 572.14 mGy.

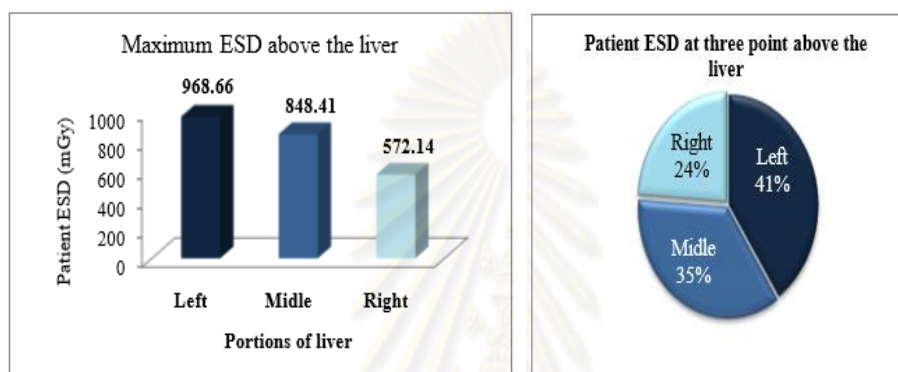


Figure 2. 13 Maximum entrance surface dose, ESD on left, middle and right lobes of liver

From this study, the left lobe of liver received the highest dose in comparison to the middle and right lobes of the liver. The left lobe received 41%, the middle lobe 35% and the right 24% respectively. The highest dose results in the superimpose of the spine and the abdominal aorta which is the area identify the selected vascular tumor. Therefore, the high density organ affected the radiation dose to the skin.

Kumkrua, C. [12] studied the patient skin dose by using radiochromic film and air kerma area product (KAP) meter methods in cardiac catheterization and interventional radiology.

The dose measurement was carried out from 64 patients who underwent the IR procedures, 21 cases for TOCE, 5 cases for PTBD, 22 cases for neurovascular interventional radiology procedure and 16 cases for PTCA.

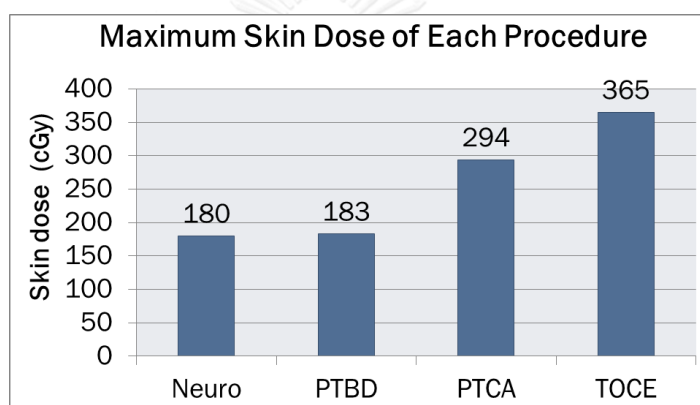


Figure 2. 14 Maximum skin dose, cGy from neurointervention, PTBD, PTCA and TOCE studies

The results showed the maximum skin dose from TOCE procedure as 365 cGy (3.65 Gy) and PTCA 294 cGy (2.94 Gy).

The result showed maximum entrance skin dose at 3.65 Gy, exceeded the threshold dose of temporary epilation of 3 Gy. The DAP meter readout maximum dose was 38,168 cGy cm^2 .

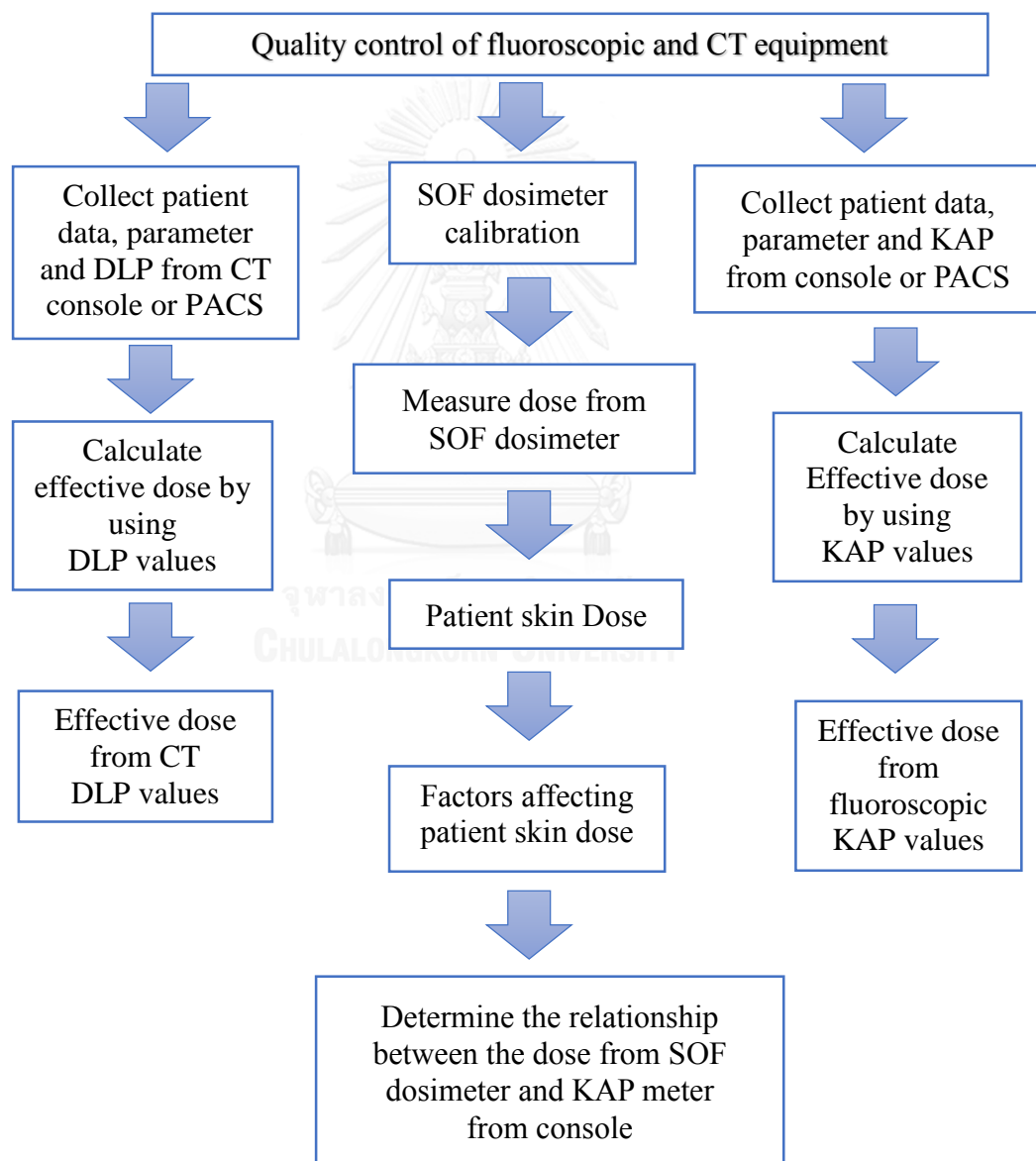
The maximum skin dose assessment from radiochromic film was greater than KAP values, because the calculated dose from KAP was the accumulated skin dose at different area and it was not the point entrance area of the patient.

CHAPTER III
RESEARCH METHODOLOGY

3.1 Research design

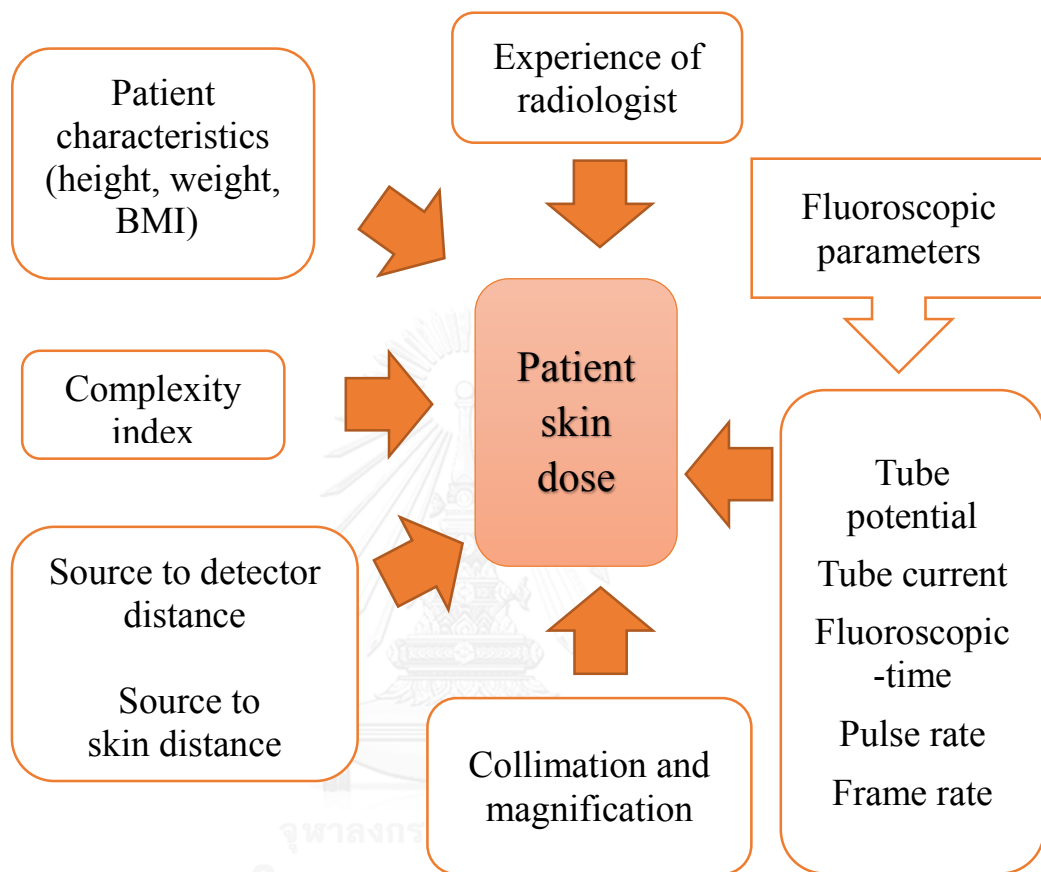
This study is an observational descriptive design (prospective study).

3.2 Research design model



3.3 Conceptual framework

Radiographic – fluoroscopic



3.4 Research question

What are patient radiation dose received from TACE and PTBD procedures measured by SOF dosimeter?

What are parameters influence the patient skin dose in TACE and PTBD procedures?

3.5 Sample

3.5.1 Target population

The patients who underwent TACE (Transarterial Chemoembolization) and PTBD (Percutaneous transhepatic biliary drainage) interventional procedures at King Chulalongkorn Memorial Hospital.

3.5.2 Sample population

This research was cross sectional descriptive study. The data was collected from the patients who underwent in TACE and PTBD procedures at Department of Radiology, King Chulalongkorn Memorial Hospital.

3.5.3 Eligible criteria

3.5.3.1 Inclusion criteria

The Hepatocellular carcinoma, HCC patients who underwent TACE procedures PTBD procedures performed in patients with obstructive jaundice using digital Flat-panel system at Interventional Radiology unit, King Chulalongkorn Memorial Hospital, on Monday to Friday from September 2016 to February 2017 consecutively.

3.5.3.2 Exclusion criteria

- Patients age < 18 years old
- Unconscious patients

3.5.4 Sample size determination

The sample population is independent, prospective data. So the sample size determined by formula,

$$\begin{aligned} N &= (Z_{\alpha/2})^2 \sigma^2 / d^2 \\ &= (1.96)^2 (1.6)^2 / (0.4)^2 \\ &= 61.46 \\ N &= 62 \end{aligned}$$

By $\alpha = 0.05$
 $Z_{\alpha/2} = 1.96$
 $d = 0.4$ Acceptable error
 $\sigma^2 = \text{Variance } 1.6$

The sample size (N) for 95% confidence interval is 62 patients.

3.6 Materials

3.6.1 Research Equipment

The Digital flat-panel radiographic- fluoroscopic system, as shown in figure 3.1 is manufactured Toshiba Medical System and installed at interventional Radiology unit, King Chulalongkorn Memorial Hospital

Radiographic –fluoroscopic system and Computed Tomography
 For Angiography system (Infinix-I 8000C FPD 12*16 inch).
 For CT system using a 16 slice (Aquilion LB) was used.



Figure 3. 1 Toshiba IVR-CT

The system comprises a KAP meter, air kerma product.

The parameters presented on the operator console are:

- Cumulative fluoroscopic time
- Cumulative air kerma product (KAP)
- Cumulative air kerma (AK)
- Total number of frames
- kV, mAs

Air kerma area product meter (KAP)

KAP meter will be used to measure the air kerma (mGy), times the area of the X-ray field (cm²), on patient skin. KAP is sometimes displayed in mGy.cm². In this study the KAP meter is installed on the collimator of the x-ray tube as shown in figure 3.2.

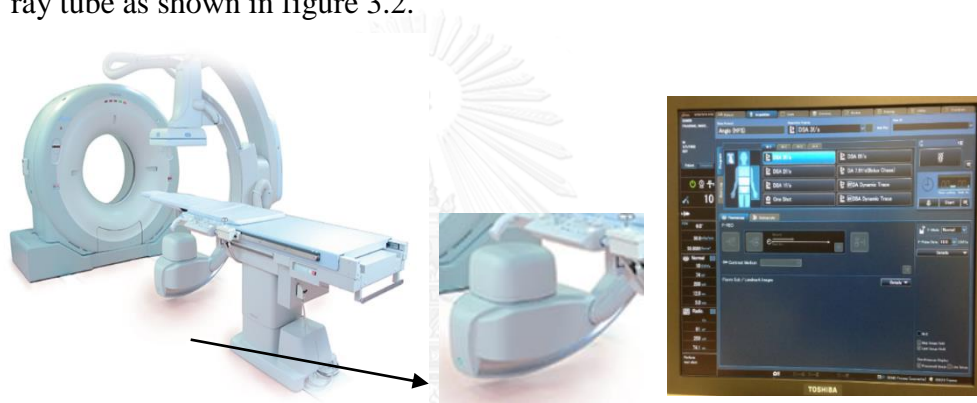


Figure 3. 2 Left: KAP meter installed on collimator of the X-ray tube.
Right: The operator console for KAP readout value.

3.6.2 Quality control materials

3.6.2.1 PMMA Phantom

The CT phantom is manufactured to comply with the FDA performance standard for diagnostic x-ray systems. The cylindrical phantom of two 14 cm lengths is made of solid Polymethyl Methacrylate (PMMA) disks measuring 16 cm (head) diameter as shown in figure 3.3 and 32 cm (body) in diameter.



Figure 3. 3 Cylindrical PMMA phantom of 16 cm diameter.

There are 5 holes with acrylic rods to plug the holes for the phantoms when not in use. Through holes are 1.31 cm in diameter and 14 cm length to accommodate standard CT probes. One is at center and four are around the perimeter, 90° apart and 1 cm hole center to the outside edge of each phantom.

3.6.2.2 Copper sheets

Copper sheets; 0.5 mm (4 sheets) and 1 mm (2 sheets) thickness were used to drive kVp during QC of fluoroscopy system.



Figure 3. 4 Copper sheets.

3.6.2.3 The chamber for computed tomography dose index (CTDI).

The 10X6-3CT is a Computed tomography dose index (CTDI) and dose length product (DLP) Chamber. Although designed specifically for CT X-ray beam measurements, either free-in-air or mounted in a head or body phantom, it can be used for DWP and DLP applications such as Dental x-ray measurements, due to the chambers excellent energy and partial volume response as well as uniformity along its entire 10 cm active length is shown in Figure 3.5.



Figure 3. 5 The 10X6-3CT Detector 10 cm length of the pencil-type ionization.

Table 3. 1 Radcal Accu-gold Digitizer module.

Solid State and Ion chamber sensors	Multiple solutions for your measurement needs, no compromising
Simultaneous measurements	Up to 16 user selectable parameters viewable from each measurement
Customizable view screens	Create data display profile either before or after the exposure
Plug and Play sensors	Truly Interchangeable Accu-Gold+ Multisensors with other Rapid-Gold+ and Accu-Gold+ meters
Real time waveforms	Real time simultaneous dose rate, kV, and mA waveforms
Data recall	Entire measurement sessions can be quickly recalled and added to at any time
Matrix display	Use Matrix display to view measurement results from the control room
Auxiliary port	Provision for future sensors
Scope type waveform analysis	Analyze kV, dose, and mA waveform measurement values in detail
Export data	Export data to Excel, user templates or clipboard

3.6.2.4 R/F dosimeter

The AGMS-D+ is a solid state kV/dose multisensor for diagnostic range measurements. A small solid state multi-parameter sensor used for single exposure and fluoroscopy. It measures dose, dose-rate, time, kVp, Half value layer (HVL), and beam filtration. It features Flash correction of dose for beam quality. (Figure 3.6)

**Figure 3. 6** The AGMS-D+ is a Solid State.

3.6.2.5 The CIRS Model 903 phantom

The CIRS Model 903 is manufactured from Polymethyl Methacrylate (PMMA) equivalent epoxy that offers the same X-ray attenuation properties as PMMA with significantly greater durability.

The overall phantom measures 25.4 cm wide x 25.4 cm long x 20.7 cm high and consists of three attenuation plates, one test object plate and a detachable stand for easy, reproducible set-up. Test objects include high-resolution copper mesh targets from 12 – 80 lines per inch, two separate contrast-detail test objects.



Figure 3. 7 CIRS Model 903 phantom

3.6.2.6 The Catphan Phantom

The Catphan 600 builds on the capabilities of the 500 model to enable maximum performance characterization of multi-slice CT's and the enhanced sensitometry measurements required for radiation therapy. The Catphan® 600 has enhanced measurement capabilities for precise measurement of thin slices and higher resolutions found in multi-slice scanners.



Figure 3. 8 Catphan Phantom

3.6.3 Miniature invisible dosimeter using scintillator with optical fiber (MIDSOF) is shown in figure 3.9



Figure 3. 9 MIDSOF and display system

3.6.4 The patients

Sixty-two patients underwent TACE and PTBD procedures will be examined by the digital flat-panel system at Interventional Radiology unit, King Chulalongkorn Memorial Hospital.

3.6.5 Data recording, complexity index and case consent forms

The patient consent (Appendix C) will be accessed before procedure. Record the patient data in data record form. The complexity indexes (Appendix D) of procedure will be accessed by interventional radiologist at the end of the procedure.

3.7 Methods

3.7.1. Perform QC in digital Flat-panel Radiographic –Fluoroscopic system according to AAPM Report No. 58, the tests consist of:

- Dose assessment
- Automatic brightness control test
- Maximum dose rate assessment
- Table attenuation
- Image size assessment
- Half value layer (HVL)
- Image quality assessment

3.7.2 Perform the quality control of CT

The quality control of CT scanner was performed following the AAPM report No.39 (1993).[13]

3.7.3 Calibrate Miniature Invisible Dosimeter using Scintillator with Optical Fiber (MIDSOF) with calibrated ion chamber

3.7.4. Data Collection

3.7.4.1. The patient consent form (Appendix C)

3.7.4.2. Record the patient data: body weight, height, age, gender, kVp, mAs, fluoroscopic time, fluoroscopic mode, frame rate, KAP (Gycm^2) and total DLP (mGycm) the case record form.

3.7.5. Dosimetric procedure

Place MIDSOF on patient's back over the liver as shown in figure 3.10

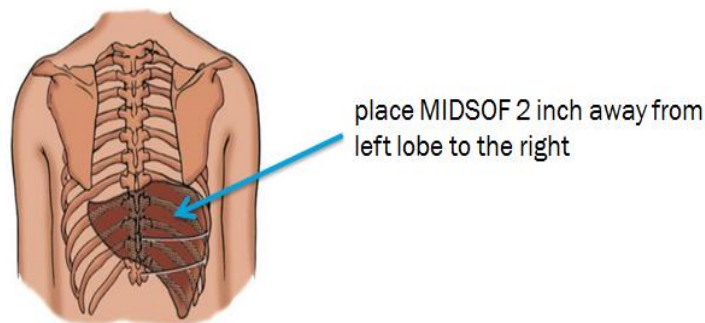


Figure 3. 10 MIDSOF placed on patient's back at a point over the liver

Left lobe : T-12

Middle lobe : place MIDSOF 2 inch away from left lobe to the right

However, fluoroscopic guide must be performed to confirm the MIDSOF position.

3.7.6 Record patient doses from MIDSOF and KAP meter in case record form.

3.7.7 Study the relationship between cumulative skin dose and exposure parameters and the relationship between cumulative skin dose from SOF dosimeter and KAP values.

3.7.8 Effective dose calculation

Calculate the effective dose by using equations;

- Effective dose (mSv) from CT = DLP (mGy.cm) \times k-factor (mSv/mGy.cm) [3] ; k-factor (Conversion factors) is 0.015 mSv/mGy.cm for CT abdomen. [14]

- Effective dose (mSv) from DSA = KAP (Gy.cm²) × Dose conversion coefficient (DCCE; mSv/Gy.cm²); DCCE is 0.26 mSv/Gy.cm² for Chemoembolization. [15]

MS excel was using for recorded the data and analyzed the mean, standard deviation, minimum and maximum of skin dose.

3.8 Variables measurement

Measure independent and dependent variables;

3.8.1 Independent variables: Interventional radiology procedures, Exposure techniques, Acquisition protocols

3.8.2 Dependent variables: KAP (Gy.cm²), patient skin dose (mGy)

3.9 Statistical analysis

3.9.1 This study is Descriptive statistics for continuous data to determine as following

Range (minimum-maximum)

Average

Median

Standard deviation (SD)

3.9.2 Correlation coefficient between the patient skin dose by MIDSOF and KAP method

3.9.3 Correlation coefficient between the patient skin dose and patient characteristics and protocols of fluoroscopic study was determined by Spearman correlation.

3.10 Data analysis

Data from patients will be reported as mean, standard deviation, minimum, maximum and range presented in form of table.

3.11 Outcomes

The patient skin dose in TACE procedure. The patient effective dose in TACE will be calculated by using the DLP from CT examination and KAP from Fluoroscopic study in each patient. The patient effective dose in PTBD is calculated by using the KAP values from Fluoroscopic study.

3.12 Expected benefits

3.12.1 The range of patient skin doses in TACE procedures.

3.12.2 Parameters influenced the patient skin dose in TACE procedures.

3.12.3 Optimization of TACE and PTBD interventional radiology procedures to obtain the correlation of patient skin dose and affecting factors.

3.12.4 The effective doses from CT and Fluoroscopic examinations are expected from this study.

These would be beneficial to the patients and the radiologists in order to justify requesting the examination or further investigations. The patient dose reduction should be considered for the radiation safety for the patients.

3.13 Limitation

Only one detector of MIDSOF or SOF dosimeter is available.

3.14 Ethical consideration

This study is performed in patients exposed by the radiography/fluoroscopic system. Patient radiation doses will be collected from the monitor of the system or PACS.

The research proposal will be submitted to the Ethic Committee, Faculty of Medicine Chulalongkorn University.

Add Belmont

Respect for persons

Respect for free and informed consent: the patient who participates in this research can decide after obtain the information.

Respect for confidential: the patient data will be for academic objective only, conceal to the public and no patient's name reveal according to the law.

Beneficence

The patient participated in this research will be informed the skin dose from TACE procedures. The patient effective dose in TACE and PTBD is obtained after completion of the research.

Justice

Selection of subjects for this research has obviously inclusion and exclusion criteria, non-bias.

CHAPTER IV

RESULT

4.1 Quality control of the DSA equipment: Toshiba, Infinix-I FPD 12*16 inch

The performance of the digital subtraction angiography equipment was evaluated including the test of electromechanical component, dose assessment, automatic brightness control test, maximum dose rate assessment, table attenuation, image size assessment, half value layer assessment and image quality assessment. The results are shown in Appendix E (page 85).

4.2 Quality control of the CT scanner: Toshiba, Aquilion LB 16 slide

The quality control of CT scanner was performed following AAPM report No.39 [20]. It includes the test of electromechanical component, image quality and radiation dose. The detail of quality control of CT scanner is shown with the summarized report of CT scanner performance test in Appendix E (page 88).

4.3 The transarterial chemoembolization (TACE) procedures patient studies.

Our study included fifty-four consecutive patients (11 women and 43 men) who underwent TACE procedure during the period July 2016 to February 2017 as shown in table 4.1. The mean age \pm SD, and range were 63.31 \pm 9.91 (46-92) years, the patient height and weight were 164.02 \pm 8.41 (143-180) cm. and 65.7 \pm 10.12 (45.6-90.0) kg, the BMI 24.43 \pm 3.48 (17.28-37.18) kg/m² respectively. Those are summarized in Table 4.2. All patients completed the consent form.

Table 4. 1 The 54 patient data underwent TACE procedure.

Patient No.	Sex (M/F)	Age (Years)	Height (cm)	Weight (kg)	BMI (kg/m ²)
1	F	68	150	59.9	26.62
2	F	66	159	64.9	25.67
3	M	69	158	58.8	23.55
4	F	71	152	85.9	37.18
5	M	54	165	66	24.24
6	F	55	160	54	21.09
7	M	74	168	66.9	23.70
8	M	60	167	81.8	29.33
9	M	62	163	62.3	23.45
10	F	80	164	71.8	26.70
11	F	92	148	45.6	20.82
12	M	64	167	69.5	24.92
13	M	60	165	65.9	24.21
14	M	60	175	59	19.27
15	M	56	164	46.5	17.29
16	M	59	170	65	22.49
17	F	87	151	56	24.56
18	M	46	170	74	25.61
19	M	66	170	66	22.84
20	M	60	160	53	20.70
21	M	70	172	70	23.66
22	M	71	156	60.4	24.82
23	M	60	177	83.3	26.59
24	M	74	155	66	27.47
25	M	50	178	60.3	19.03
26	M	63	175	54	17.63
27	M	74	161.5	72.4	27.76

Table 4.1 The 54 patient data underwent TACE procedure. (cont.)

Patient No.	Sex (M/F)	Age (Years)	Height (cm)	Weight (kg)	BMI (kg/m ²)
28	M	62	163	71.1	26.76
29	M	51	178	78.8	24.87
30	F	70	156	52	21.37
31	M	60	172	63	21.30
32	M	63	156	63.4	26.05
33	M	61	168	59.2	20.98
34	M	56	165	65	23.88
35	M	66	180	79	24.38
36	M	52	161	58	22.38
37	M	69	157	62	25.15
38	M	65	165	80	29.38
39	F	69	143	52.6	25.72
40	M	59	170	80	27.68
41	M	46	178	78.8	31.14
42	M	46	170	90	31.14
43	M	74	162	55	20.96
44	F	58	152	53	22.94
45	F	73	153	65.3	27.90
46	M	72	165	79.9	29.35
47	M	47	175	69.1	22.56
48	M	60	162	62	23.62
49	M	80	159	64.9	25.67
50	M	56	162	55.7	21.22
51	M	52	166	62.8	22.79
52	M	60	164	80	29.74
53	M	69	175	67	21.88
54	M	52	160	61	23.83

Table 4. 2 The summary of patient data underwent TACE procedure.

patient data	Mean \pm SD	Range
Age (years)	63.31 \pm 9.91	46-92
Height (cm)	164.02 \pm 8.41	143-180
Weight (kg)	65.7 \pm 10.12	45.6-90
BMI (kg/m ²)	24.4 \pm 3.5	17.3-37.2

4.4 Average values of technical parameters.

Average values of the technical parameters used to perform the fluoroscopy part of TACE procedure are given in table 4.3

Table 4. 3 Mean values of technical parameters.

TACE Procedure	Mean \pm SD	range
kVp	71 \pm 10	70-120
mA	109 \pm 55	32-200
ms	7.7 \pm 2.1	4.7-12
FOV	6" -16"	
mode	Normal	
Frame rate (Exp/s)	10	
Filter	Cu 0.3 mm	

4.5 Procedure performed with a Flat-panel system (Toshiba)

The parameters in TACE procedure such as fluoroscopic time, number of frames, number of procedures and frame rate. Those factors are shown in table 4.4

The average fluoroscopic time was 2000 ± 905 second with the range of 554-4257 second. The average total acquisition time was 93.84 ± 33.74 s. The average number of frames was 200.3 ± 84.4 , and the range was 87-584 frames. The number of procedures was 2.1 ± 1.9 range 1-10 procedures.

The procedures were performed by four experienced radiologists using standard techniques. Every case was attended by a physician training. The average experience of interventional radiologists from 54 cases was 4.7 ± 0.7 years with the range was 3-5 years. From all samples that has been taken, only one case that was diagnostic type of procedure as shown in table 4.5

Table 4. 4 The patient data performed with a digital flat-panel system (Infinix-I 8000C FPD 12*16 inch) in TACE procedure.

Patient No.	Total Fluoroscopic Time (s)	Total Acquisition Time (s)	Total Number of Frames	Number of procedure (time)	Experience of radiologist (year)
1	1455	71.92	156	10	5
2	2006	74.86	161	1	5
3	2284	50.09	104	1	5
4	1004	61.41	124	3	5
5	2373	178.94	584	2	5
6	1777	104.20	227	2	5
7	1698	59.63	124	2	5
8	832	83.59	174	2	5
9	2283	64.02	139	2	5
10	3574	61.75	131	1	5

Table 4.4 The patient data performed with a Digital Flat-Panel system (Infinix-I 8000C FPD 12*16 inch) in TACE procedure. (cont.)

Patient No.	Total Fluoroscopic Time (s)	Total Acquisition Time (s)	Total Number of Frames	Number of procedure (time)	Experience of radiologist (year)
11	2701	116.39	278	2	5
12	1157	75.65	164	1	5
13	4066	102.67	206	3	5
14	1404	90.00	194	3	5
15	1347	73.58	155	7	5
16	2509	82.74	174	2	5
17	2321	87.50	165	1	5
18	1311	90.52	187	1	5
19	1840	115.75	219	1	5
20	3261	98.51	189	1	5
21	1848	65.11	131	3	5
22	2898	75.98	155	2	5
23	3053	171.44	361	6	3
24	1128	50.70	112	2	3
25	1196	84.83	181	3	5
26	1487	60.20	129	1	5
27	2443	111.26	222	1	5
28	2728	141.27	307	6	3
29	1170	86.17	187	1	5
30	4257	108.86	232	1	5
31	1093	67.50	151	3	5
32	2897	128.63	262	2	5
33	1942	80.79	168	1	3
34	1440	136.63	287	4	3
35	1531	81.35	171	3	5

*number of procedure - mean number of patients repeated the procedure

Table 4.4 The procedures performed with a Digital Flat-Panel system (Infinix-I 8000C FPD 12*16 inch) in TACE procedure. (cont.)

Patient No.	Total Fluoroscopic Time (s)	Total Acquisition Time (s)	Total Number of Frames	Number of procedure (time)	Experience of radiologist (year)
36	1275	63.84	140	1	5
37	1590	59.67	127	5	5
38	1923	126.72	275	6	3
39	1975	104.41	208	4	5
40	1456	114.41	262	1	5
41	1104	62.86	136	1	5
42	970	65.32	144	1	3
43	738	102.43	210	1	5
44	554	49.01	106	2	5
45	1725	93.42	188	2	5
46	2181	148.96	332	2	5
47	1984	39.65	87	2	5
48	3198	104.13	218	1	3
49	1445	101.69	207	1	5
50	3277	85.77	174	2	5
51	2812	152.16	312	6	5
52	4175	152.52	304	2	5
53	652	69.67	146	1	5
54	2702	176.46	358	2	5

Table 4.5 The factors affecting patient dose in TACE procedure.

Factors affecting	Mean \pm SD	Range
Total Fluoro Time (s)	2000 \pm 905	554-4257
Total Acquisition Time (s)	93.84 \pm 33.74	39.6-178.9
Total Number of Frames	200 \pm 84	87-584
Number of procedures	2 \pm 2	1-10
Experience of radiologist (Years)	5 \pm 1	3-5

4.6 The total air kerma product (Gycm^2) and patient skin dose determined by MIDSOF (Gy) of TACE procedure shown in table 4.6.

The total average dose air kerma product from KAP meter readout was $379.88 \pm 147.78 \text{ Gycm}^2$ and the range was $59.9 - 725.2 \text{ Gycm}^2$

The average patient skin dose determined by MIDSOF was $1.71 \pm 1.14 \text{ Gy}$ and the range was $0.023 - 5.48 \text{ Gy}$.

Table 4. 6 The total dose air kerma product (Gycm^2) and patient skin dose determined by MIDSOF (Gy) and system detector on TACE procedure.

Patient No.	Total dose air kerma Product (Gycm^2)	Total fluoro dose air kerma product (Gycm^2)	Total acquisition dose air kerma product (Gycm^2)	Total dose (Gy)	Dose from MIDSOF (Gy)
1	206	125	80	1.18	1.88
2	233	100	64	2.16	2.78
3	114.1	86.5	27.8	0.65	1.47
4	193	105	88	0.81	1.91
5	365	143	222	2.41	2.48
6	78.1	37	40	0.42	0.68
7	371	240	130	2.72	1.75
8	205	98	107	0.88	1.33
9	267	219	47	2.11	1.60
10	703	591	111	5.52	5.48
11	156	105.1	51	1.35	1.58
12	179	82	96	0.75	1.38
13	471	352	118	5.03	5.44
14	152	68	83	0.61	1.63
15	110	57	52	0.47	1.06
16	470	350	120	3.66	2.33
17	163	106.6	56	1.99	1.06
18	238	134	104	2.03	1.83
19	385.5	223	162	2.92	2.51
20	220	162	58	1.69	2.38

Table 4.6 The total dose air kerma product (Gycm²) and patient skin dose determined by MIDSOF (Gy) and system detector on TACE procedure. (cont.)

Patient No.	Total dose air kerma product (Gycm ²)	Total fluoro dose air kerma product (Gycm ²)	Total acquisition dose air kerma product (Gycm ²)	Total dose (Gy)	Dose from MIDSOF (Gy)
21	278.0	187.0	91.2	2.14	0.58
22	303.9	244.0	59.1	2.81	1.95
23	451.5	287.2	164.3	2.43	1.89
24	157.8	98.4	59.3	1.01	0.14
25	103.0	53.0	49.8	0.64	0.02
26	113.4	69.0	43.4	0.86	1.13
27	347.4	240.0	106.6	2.67	4.69
28	327.4	198.3	129.0	2.41	1.77
29	157.0	91.0	66.0	1.07	1.31
30	336.9	259.0	77.4	2.26	2.61
31	156.0	88.1	68.6	0.84	0.56
32	333.0	230.0	103.0	2.28	1.19
33	142.8	82.0	60.7	0.84	0.76
34	280.0	127.0	153.0	1.88	1.30
35	336.0	234.0	101.0	3.11	1.39
36	133.9	81.0	52.6	1.08	0.63
37	166.0	113.0	53.7	1.23	1.80
38	418.8	216.9	201.0	2.62	1.59
39	239.7	149.7	89.9	1.98	1.58
40	431.9	194.6	237.3	1.87	0.74
41	176.6	91.5	85.0	1.66	0.42
42	321.2	151.2	169.9	1.60	1.46
43	186.1	60.3	125.0	1.03	0.99
44	59.9	24.2	35.7	0.33	0.60
45	312.7	201.7	111.1	2.56	1.27
46	637.7	326.3	311.3	4.11	1.92
47	149.4	111.1	38.3	1.03	1.49
48	370.5	280.0	90.1	3.06	2.71
49	208.9	121.0	87.9	1.04	1.13
50	214.0	168.2	463.9	2.59	0.83

Table 4.6 The total dose air kerma product (Gycm^2) and patient skin dose determined by MIDSOF (Gy) and system detector on TACE procedure. (cont.)

Patient No.	Total dose air kerma product (Gycm^2)	Total fluoro dose air kerma product (Gycm^2)	Total acquisition dose air kerma product (Gycm^2)	Total dose (Gy)	Dose from MIDSOF (Gy)
51	257.9	147	110.4	2.07	1.61
52	725.2	493.8	231.4	5.76	3.22
53	153.3	66	87.3	1.17	0.43
54	451.1	248.9	202.1	2.61	4.00

4.7 The effective dose was determined by KAP method in TACE procedures during the procedure to identify the selected vascular supply tumor. The effective dose determined by DLP from CT is shown in table 4.7.

After collecting patient data and scanning parameters, the effective dose from fluoroscopic procedures was calculated by using $\text{KAP (Gy.cm}^2) \times \text{Dose conversion coefficient (0.26 mSv/Gy.cm}^2)$. [15]

The effective dose of CT was calculated using $\text{DLP (mGy.cm)} \times \text{k-factor (mSv/mGy.cm)}$. For CT abdomen, k-factor was 0.015 mSv/mGy.cm.[14]

The average dose length product (DLP) of CT system was 462.56 ± 204 mGy.cm. The range was 212 – 1,364 mGy.cm.

Table 4. 7 The effective dose determined by KAP method and the effective dose determined by DLP in TACE procedure.

Patient No.	KAP meter readout (Gycm ²)	Conversion coefficient (mSv/Gy.cm ²)	Effective dose (mSv)	DLP total (mGy.cm)	Effective dose (mSv)
1	206	0.26	53.6	333.6	5.0
2	233	0.26	60.6	381.1	5.7
3	114	0.26	29.7	614.4	9.2
4	193	0.26	50.2	490.2	7.4
5	365	0.26	94.9	676.8	10.2
6	78	0.26	20.3	435.5	6.5
7	371	0.26	96.5	614.4	9.2
8	205	0.26	53.3	1144	17.2
9	267	0.26	69.4	523.9	7.9
10	703	0.26	182.8	400	6.0
11	156	0.26	40.6	295.8	4.4
12	179	0.26	46.5	402.3	6.0
13	471	0.26	122.5	490.2	7.4
14	152	0.26	39.5	452.7	6.8
15	110	0.26	28.6	316.9	4.8
16	470	0.26	122.2	561	8.4
17	163	0.26	42.4	303.3	4.5
18	238	0.26	61.9	532.6	8.0
19	386	0.26	100.2	370.4	5.6
20	220	0.26	57.2	354	5.3
21	278	0.26	72.3	357.9	5.4
22	304	0.26	79.0	354	5.3
23	452	0.26	117.4	716.3	10.7
24	158	0.26	41.0	593.9	8.9
25	103	0.26	26.8	315.6	4.7
26	113	0.26	29.5	221.6	3.3
27	347	0.26	90.3	825.6	12.4
28	327	0.26	85.1	390.1	5.9
29	157	0.26	40.8	411.6	6.2
30	337	0.26	87.6	566.9	8.5

Table 4.7 The effective dose determined by KAP method and the effective dose determined by DLP in TACE procedure. (cont.)

Patient No.	KAP meter readout (Gycm ²)	Conversion coefficient (mSv/Gy.cm ²)	Effective dose (mSv)	DLP total (mGy.cm)	Effective dose (mSv)
31	40.6	0.26	10.5	228.9	3.4
32	86.6	0.26	22.5	554.3	8.3
33	37.1	0.26	9.7	357.8	5.4
34	72.8	0.26	18.9	524.2	7.9
35	87.4	0.26	22.7	478.7	7.2
36	34.8	0.26	9.1	304.2	4.6
37	43.2	0.26	11.2	212.9	3.2
38	108.9	0.26	28.3	368.3	5.5
39	62.3	0.26	16.2	333.3	5.0
40	112.3	0.26	29.2	368.3	5.5
41	45.9	0.26	11.9	357.7	5.4
42	83.5	0.26	21.7	552.2	8.3
43	48.4	0.26	12.6	427.8	6.4
44	15.6	0.26	4.0	287.3	4.3
45	81.3	0.26	21.1	365.1	5.5
46	165.8	0.26	43.1	1364.9	20.5
47	38.8	0.26	10.1	418.5	6.3
48	96.3	0.26	25.0	484.4	7.3
49	54.3	0.26	14.1	364.3	5.5
50	55.6	0.26	14.5	373.8	5.6
51	67.1	0.26	17.4	428.7	6.4
52	188.6	0.26	49.0	725.1	10.9
53	39.9	0.26	10.4	392.8	5.9
54	117.3	0.26	30.5	258.2	3.9

The average effective dose of fluoroscopic system was 70.86 mSv. The range was 15.57-188.55 mSv. The average effective dose from CT was 6.93 mSv and the range was 3.19 - 20.47 mSv. The effective dose from both systems of each patient was plotted as shown in figure 4.1

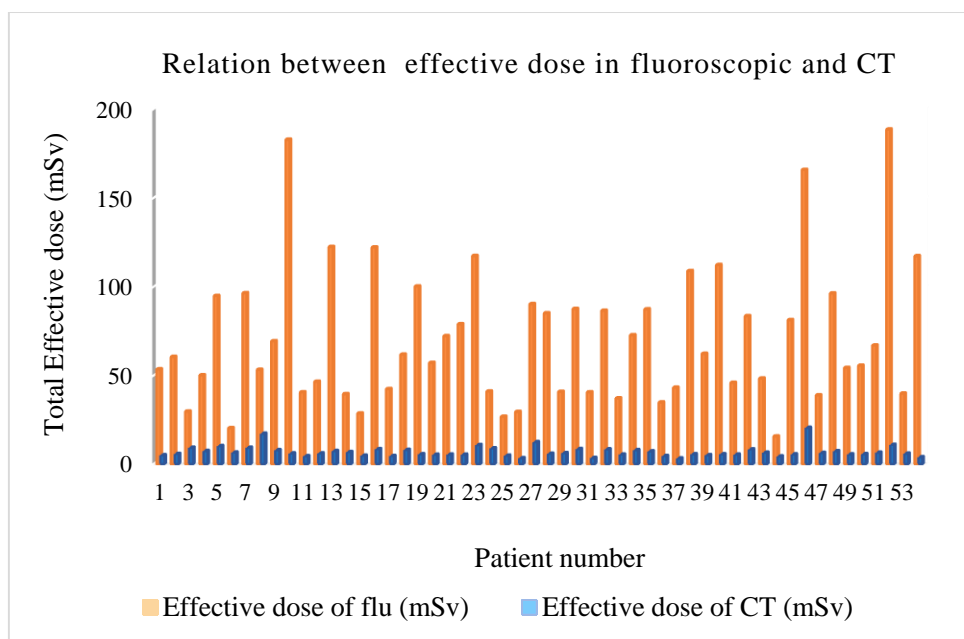


Figure 4. 1 The effective dose in TACE patients using fluoroscope and CT procedures

4.8 The Complexity index

The complexity index of each procedure from fifty-four cases was recorded by the interventional radiologist. The data of complexity index was shown in APPENDIX D (page 79)

4.9 The correlation between the dose air kerma product, KAP (Gycm^2) and patient skin dose determined by MIDSOF (Gy) of TACE procedure.

The correlation between the dose air kerma product, KAP (Gycm^2) and patient skin dose determined by MIDSOF (Gy) of TACE procedure is displayed in figure 4.2.

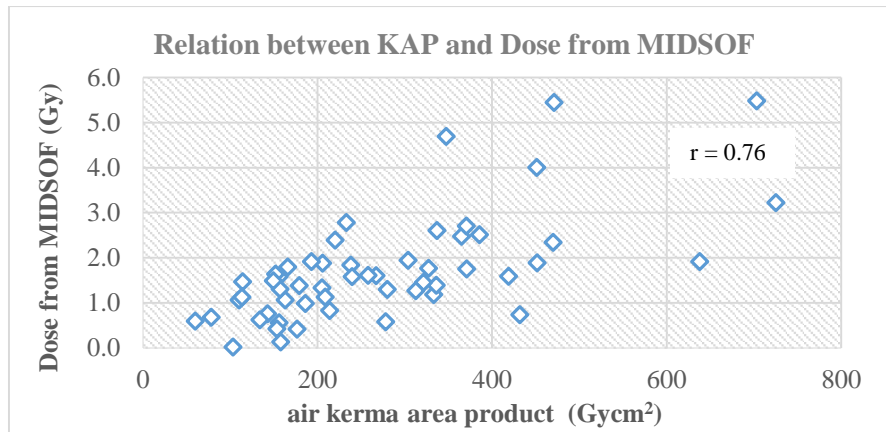


Figure 4. 2 The correlation between the dose air kerma product, KAP (Gycm^2) and patient skin dose determined by MIDSOF (Gy) from 54 cases in TACE procedure with $r = 0.76$.

4.10 The relation between patient skin dose determined by MIDSOF (Gy) and the affecting factor in TACE procedure.

The scatter diagrams show the relation between the patient skin dose determined by MIDSOF (Gy) and the fluoroscopic time as in figure 4.3 the relation between patient skin dose determined by MIDSOF (Gy) and total number of radiographic frames is shown in figure 4.4

4.10.1 The relation between the patient skin dose determined by MIDSOF (Gy) and the fluoroscopic time.

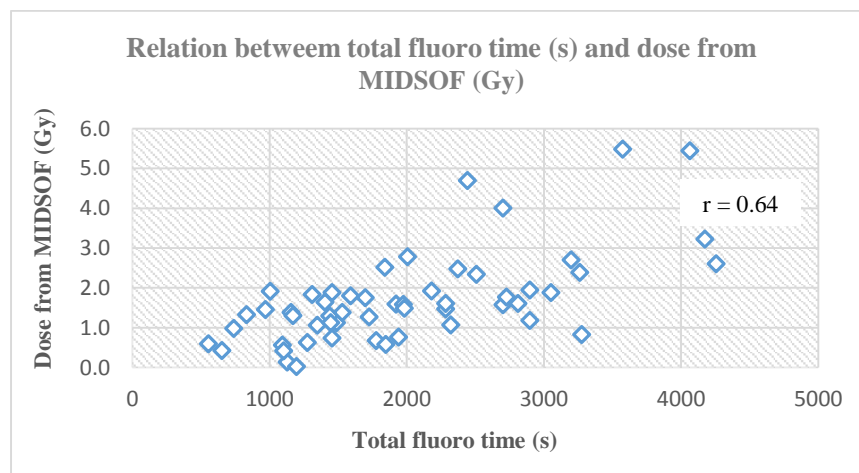


Figure 4. 3 The relation between the patient skin dose determined by MIDSOF (Gy) and the fluoroscopic time in second.

4.10.2 The relation between the patient skin dose determined by MIDSOF (Gy) and total number of radiographic frames.

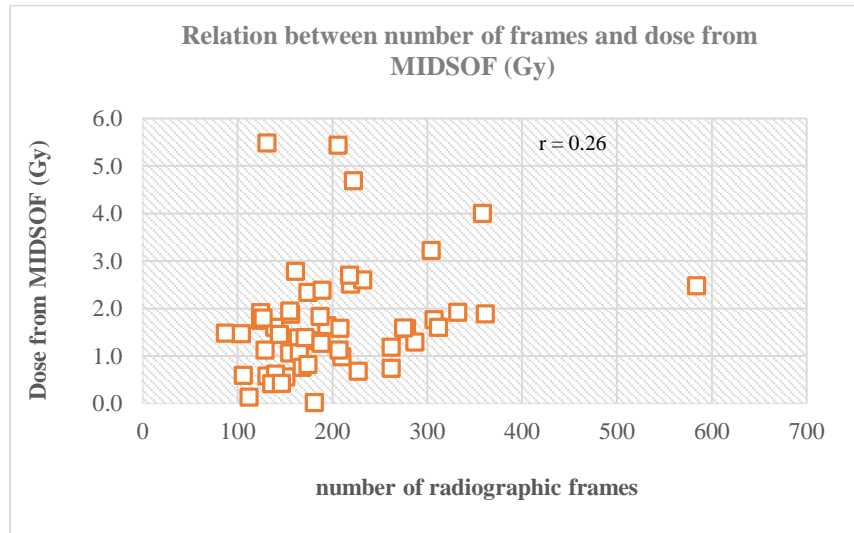


Figure 4. 4 The relation between the patient skin dose determined by MIDSOF (Gy) and total number of radiographic frames.

4.10.3 The relation between the patient skin dose determined by MIDSOF (Gy) and the patient BMI (kg/m^2).

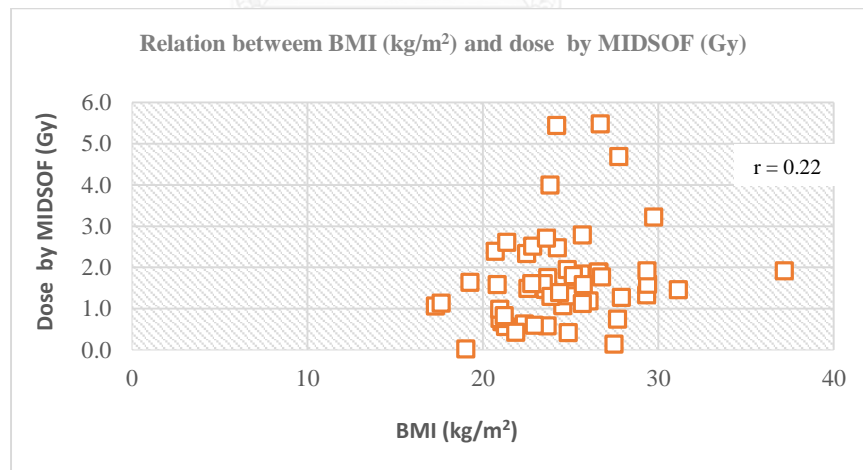


Figure 4. 5 The relation between the patient skin dose determined by MIDSOF (Gy) and the patient BMI (kg/m^2).

4.10.4 The relation between the patient skin dose determined by MIDSOF (Gy) and the experience of interventional radiologists.

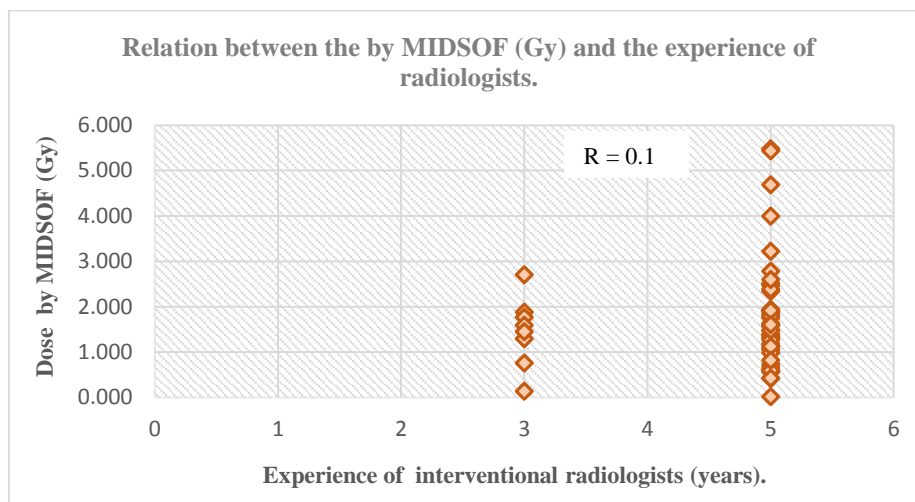


Figure 4. 6 The relation between the patient skin dose determined by MIDSOF (Gy) and the experience of interventional radiologists.

4.11 The percutaneous transhepatic biliary drainage (PTBD) patient studies.

Our study included eight consecutive patients (2 women and 6 men) who underwent PTBD procedure during the period July 2016 to February 2017 as shown in table 4.8. The mean age was 63 ± 12 (38-80) years.

The average fluoroscopic time was 305 ± 272 second with the range of 13 -926 second. The average total Acquisition Time was 3.35 ± 1.6 second with the range of 1.38 – 7.5 second. The average number of frames was 4 ± 1 frames with the range of 2 – 5.

The total average dose air kerma product from KAP meter readout was 21.9 ± 26.9 Gy cm^2 and the range was 1.67 - 87 Gy cm^2 . The average effective dose was 5.69 ± 7.01 mSv and the range was 0.43– 22.6 mSv. The average patient dose was 0.14 ± 0.21 Gy and the range was 0.004 - 0.7 Gy.

Table 4. 8 The patient data underwent PTBD procedure from 8 patients.

Patient No.	Total fluoro time (s)	Total number of frames	Total dose air kerma product (Gycm ²)	Total dose (mGy)	Effective dose (mSv)
1	129	4	8.68	42.90	2.26
2	926	3	87.14	708.70	22.66
3	362	5	9.27	90.50	2.41
4	216	5	5.75	41.00	1.50
5	457	5	27.67	95.23	7.19
6	13	2	1.84	4.86	0.48
7	65	4	1.67	13.51	0.43
8	276	4	33.3	135.90	8.66

4.12 The relation between patient skin dose determined by MIDSOF (Gy) and the affecting factor in PTBD procedures.

4.12.1 The scatter diagrams show the relation between the patient skin dose (Gy) and the air kerma area product, KAP (Gycm²) as in figure 4.7 the relation between patient dose (Gy) and the fluoroscopic time is shown in figure 4.8

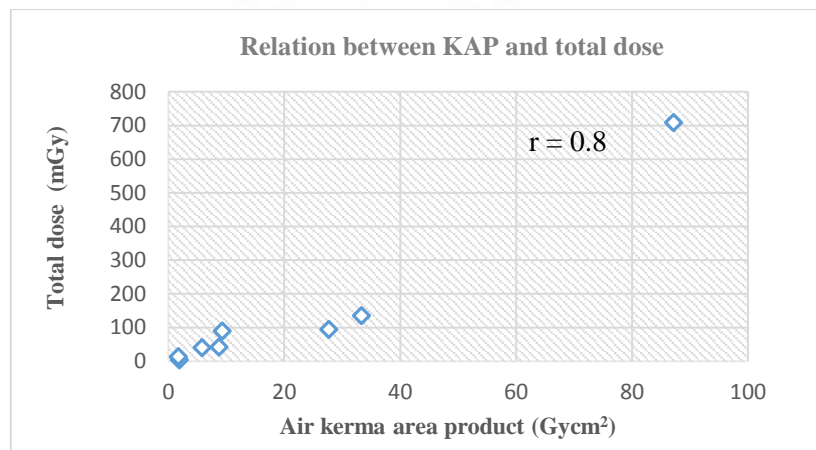


Figure 4. 7 The correlation between the dose air kerma product, KAP (Gycm²) and patient dose (mGy) from 8 cases in PTBD procedure with $r = 0.8$.

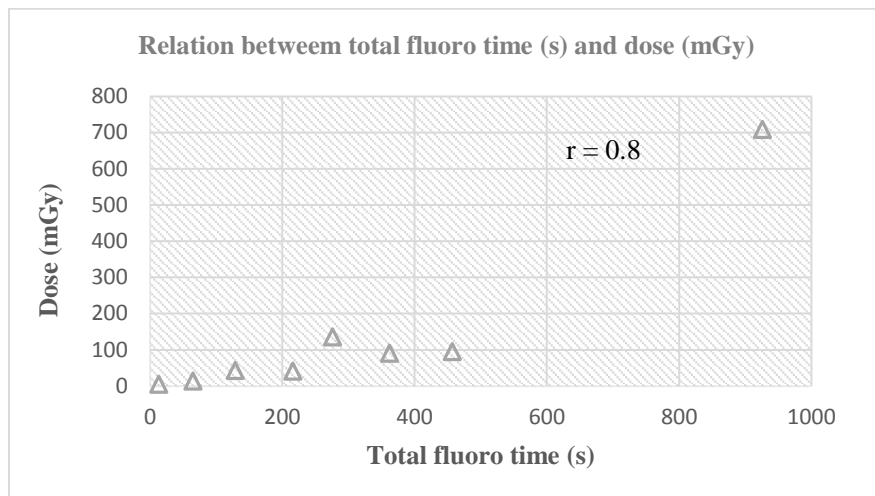


Figure 4. 8 The relation between the patient skin dose (mGy) and the fluoroscopic time in second.

4.12.2 The relation between the patient skin dose (mGy) and total number of radiographic frames.

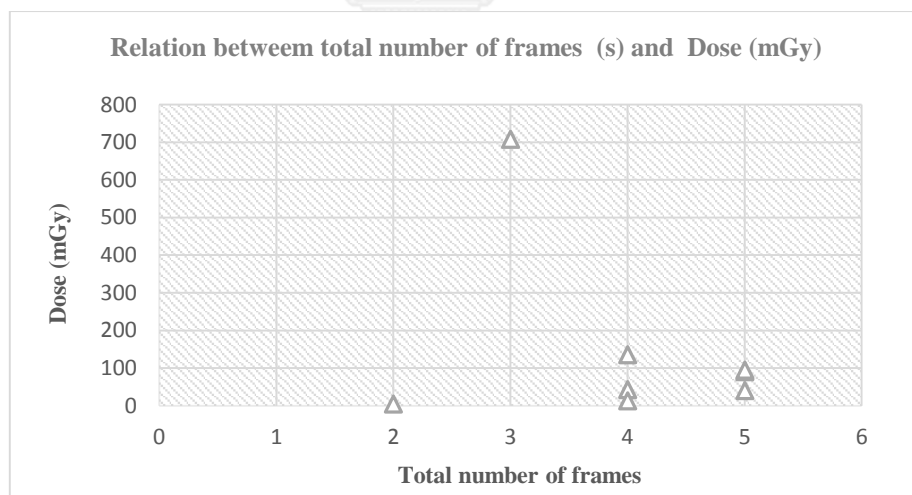


Figure 4. 9 The relation between the patient skin dose (mGy) and total number of frames.

4.12.3 The effective dose from 8 cases in PTBD procedures. The average effective dose was 5.69 ± 7.01 mSv and the range was 0.43– 22.6 mSv.

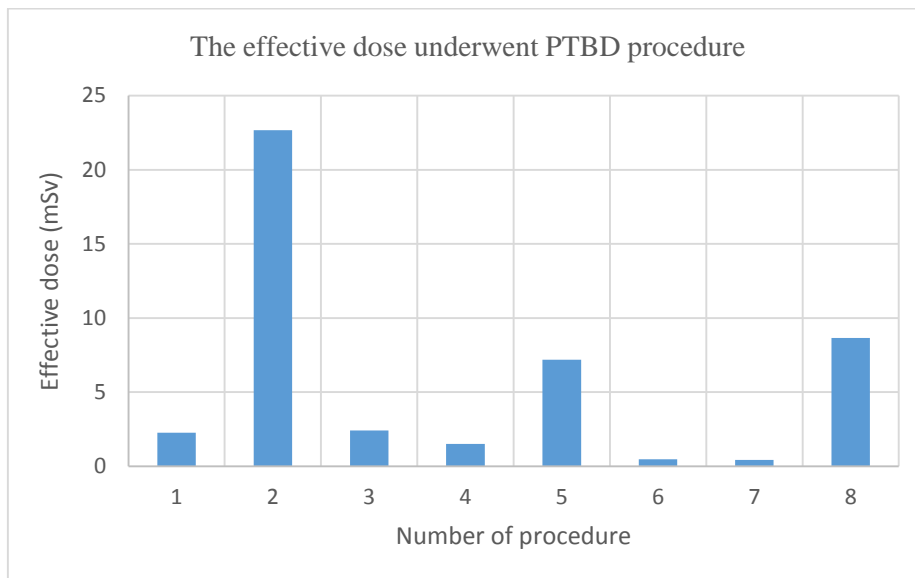


Figure 4. 10 The effective dose underwent PTBD procedure from 8 patients



CHAPTER V

DISCUSSION AND CONCLUSION

5.1 Discussion

5.1.1. The patients

Transarterial chemoembolization (TACE) procedures.

Our study included fifty-four consecutive patients (11 women and 43 men) who underwent TACE procedures. The mean age, \pm SD and range were 63.31 ± 9.91 (46-92) years, the patient height and weight were 164.02 ± 8.41 (143-180) cm. and 65.7 ± 10.12 (45.6-90) kg, the BMI 24.43 ± 3.48 (17.28-37.18) kg/m^2 respectively.

The patient who received the highest skin dose was 80 year old female. This procedure was her second TACE procedures. The CT procedure was performed to identify the selected vascular.

The cumulative fluoroscopic time was 60 min. The number of frames for fluoroscopy was 131 frames. The KAP meter readout was $703 \text{ Gy}\cdot\text{cm}^2$. The effective dose for Angio-CT was 188.78 mSv.

Percutaneous transhepatic biliary drainage (PTBD) procedures.

Our study included eight consecutive patients (2 women and 6 men) who underwent PTBD procedures. The mean age and range were 63 ± 12 (38-80) years.

The patient who received the highest skin dose at 0.7 Gy, the cumulative fluoroscopic time was 15 min, the KAP meter readout was $87 \text{ Gy}\cdot\text{cm}^2$, the number of frames was 3 frames and the effective dose was 22.6 mSv.

In TACE procedure, twelve from fifty four patients received the skin dose exceed the level for transient erythema (2 Gy) measured by MIDSOF as in table 5.1.

Table 5. 1 The patients who received the skin dose exceed the transient erythema.

Date	HN	Dose from MIDSOF (Gy)	Dose from monitor (Gy)
21/7/2559	9939/59	5.48	5.51
25/7/2559	30544/58	5.40	5.00
9/8/2559	57353/59	4.60	3.00
14/2/2560	54090/48	4.00	2.70
7/2/2560	5843/50	3.30	5.70
7/7/2559	15343/56	2.78	2.16

Table 5. 1 The patients who received the skin dose exceed the transient erythema (cont.)

Date	HN	Dose from	Dose from
		MIDSOF (Gy)	monitor (Gy)
3/2/2560	8694/57	2.71	3.06
18/10/2559	82248/59	2.61	2.26
28/7/2559	82315/58	2.52	2.92
11/7/2559	1324/59	2.48	2.41
28/7/2559	21184/58	2.39	2.00
26/7/2559	49040/58	2.34	3.66

Table 5. 2 Tissue reaction from single-delivery radiation dose to skin

tissue Reactions from Single-Delivery Radiation Dose to skin of the neck, Torso, Pelvis, Buttocks, or Arms						
Band	Single-site Acute Skin-Dose Range(Gy)*	NCI Skin Reaction Grade	Approximate Time of Onset of Effects			
			Prompt	Early	Midterm	Long Term
A1	0-2	NA	No observable effects expected	No observable effects expected	No observable effects expected	No observable effects expected
A2	2-5	1	Transient erythema	Epilation	Recovery from hair loss	No observable effects expected
B	5-10	1-2	Transient erythema	Erythema, epilation	Recovery; at high doses, prolonged erythema, permanent partial epilation	Recovery; at higher doses dermal atrophy or induration
C	10-15	2-3	Transient erythema	Erythema, epilation; possible dry or moist desquamation; recovery from desquamation	prolonged erythema; permanent epilation	Telangiectasia; dermal atrophy or induration; possible late skin breakdown; wound might
D	> 15	3-4	Transient erythema; after very high doses, edema and acute ulceration; long-term surgical intervention likely to be required	Erythema, epilation; moist desquamation	Dermal atrophy; secondary ulceration due to failure of moist desquamation to heal; surgical interventional likely to be required; at higher doses, dermal necrosis, surgical intervention likely to be required	be persistent and progress into a deeper lesion; surgical intervention likely to be required

Note - Applicable to normal range of patient radiosensitivities in absence of mitigating or aggravating physical or clinical factors. Data do not apply to the skin of the scalp. Dose and time bands are not rigid boundaries. Signs and symptoms are expected to appear earlier as skin dose increases. Prompt is < 2 weeks; early, 2-8 weeks; midterm, 6-52 weeks; long term, > 40 weeks. *Skin dose refers to actual skin dose (backscatter). This quantity is not the reference point air kerma described by Food and Drug Administration (21 CFR 1020.32[2008]) or International Electrotechnical Commission (57). Skin dosimetry is unlikely to be more accurate than $\pm 50\%$ NA = not applicable
 NCI = National Cancer Institute Refers to radiation-induced. Telangiectasia associated with area of initial moist desquamation or healing of ulceration may be present earlier.

(source Balter et al. Fluoroscopically Guided Interventional Procedures: A Review of Radiation Effects on Patients' Skin and Hair. Radiology: Volume 254: Number 2 February 2010)

Table 5. 3 Five bands of patient skin dose measured by MIDSOF and by system detector (Gy)

Band	Single-site Acute Skin-Dose Range(Gy)*	NCI Skin Reaction Grade	Dose from MIDSOF (Gy)	Number of patient received the skin dose	Dose from monitor (Gy)	Number of patient received the skin dose
A1	0-2	NA	0-2	42	0-2	30
A2	2-5	1	2-5	10	2-5	22
B	5-10	1-2	5-10	2	5-10	2
C	10-15	2-3	10-15	-	10-15	-
D	> 15	3-4	> 15	-	> 15	-

From MIDSOF record, 42 patients received skin dose less than 2 Gy, 10 patients received skin dose between 2 and 5 Gy and 2 patients received skin dose between 5 and 10 Gy. Twelve patients had the risk of epilation an erythema at early stage. From the monitor record, 30 patients received the skin dose less than 2 Gy. 22 patients received the skin dose between 2 and 5 Gy, 2 patients received the skin dose between 5 to 10 Gy.

International Commission on Radiation Protection, ICRP recommended that the patient absorbed dose exceed 1 Gy must be recorded. 41 from 62 patients received the skin dose higher the ICRP recommendation.

5.1.2. Comparison of the result with other studies

The result was compared with previous studies as shown in table 5.4. Our study shows the second highest fluoroscopic time of 70 minutes while the KAP was third highest of 725 Gy cm^2 after Svetlana S et al. of 855 Gy cm^2 and E.Vano et al. of 830 Gy cm^2 .

Table 5. 4 Comparison of KAP readouts with other studies during TACE procedure.

Author	year	country	Detector system	No. of patient	Fluoroscopic time (min)		KAP (Gy cm^2)	
					Mean	Range	Mean	Range
Kumkrue [12]	2004	Thailand	II	21	NA	2.4-4.8	NA	24.3-381.6
B Sapiin [16]	2004	Malaysia	NA	6	29.7 \pm 4.6	19.6-45.9	127	30-237.9
BOR D [17]	2004	Turkey	II	5	3.2	1-4.7	52	3-167
S Suzuki [18]	2005	Japan	FPD	25	17.9	NA	73	36.9-133.3
Eliseo Vano [19]	2009	Spain	NA	151	19.8 \pm 1.1	2.8-80	216 \pm 176	27.4-830
E.papageorgiou [20]	2010	Greece	FPD	25	10.5 \pm 8.4	1.3-29.4	136 \pm 83	15-341
Svetlana Set [21]	2010	Russia	FPD	49	2 \pm 2.1	0.2-9.8	233 \pm 221	16-855
Sitthiphan, P. [11]	2010	Thailand	FPD	69	16	3.38-59.1	222 \pm 114	22.5-537.4
This study	2016	Thailand	FPD	54	33.3 \pm 15	10.0 -70	379 \pm 147	59.9 -725.2

II Image intensifier detector, FPD; Flat-panel detector system

5.1.3. Factors affecting radiation dose

Transarterial chemoembolization (TACE) procedures.

5.1.3.1 Air Kerma Area Product (KAP)

The patient skin dose is increasing as the KAP increases for each procedure. Table 4.6 and figures 4.2 showed KAP meter readout and the correlation with the average patient skin dose for TACE procedures. The average KAP \pm SD and range were 379.88 ± 147.78 (59.9 – 725.2) Gycm^2 .

The result shows the linear correlation between the estimated dose from KAP and the skin dose from MIDSOF with good correlation of 0.76. The KAP is estimated from the average radiation area, and the patient skin dose was measured on real exposed in air.

5.1.3.2 The fluoroscopic time

The patient skin dose is increasing as the fluoroscopic time increases for each procedure as in table 4.4 and 4.5. Figures 4.3 shows fluoroscopic time and the correlation with the average patient skin dose for TACE procedures. The average, SD and range of fluoroscopic time were 33.3 ± 15 (10- 70) min. The correlation between patient skin dose and fluoroscopic time is $r = 0.64$.

5.1.3.3 Patient BMI

The body mass index (BMI) of patient undergoing TACE procedures is shown in Table 4.1 and 4.2. The patient skin dose increases with increasing BMI for TACE procedures.

The average, \pm SD and range of BMI were 24.43 ± 3.48 (17.28 - 37.18) kg/m^2 . Figure 4.5 show the correlation between patient skin dose and patient BMI was poor correlation at $r = 0.22$. The maximum BMI was found in TACE procedure of 37.18 kg/m^2 . The body mass index of a patient is also weakly related to the risk for high skin dose in the TACE procedures in this study. This mean that the size of a patient is less important predictor of the dose delivered than other factors.

5.1.3.4 The number of frames

The number of frames in this study was shown in Table 4.4 and 4.5. Figure 4.4 showed the correlation between patient skin dose and the number of frames. The patient skin dose and the number of frames was poor correlation ($r = 0.26$).

5.1.3.5 The experience of the radiologist

The mean experience the radiologist was 4.7 ± 0.7 years with the range of 3-5 years as shown in Table 4.4. Figure 4.6 the correlation between the average patient skin dose and the experience of the radiologist was poor ($r = 0.1$).

The experience of the radiologist is a major factor in dose management but showing poor correlation with the patient skin dose. Fellow training in interventional procedures could cause a significant increase in patient exposure during fluoroscopy according the lack of experience in performing the procedure. Exposure could be further reduced by limiting the number of procedures performed by interventional radiology fellows. It would be important to decide if an interventional radiology fellow should receive enough practical training.

Percutaneous transhepatic biliary drainage (PTBD).

5.1.3.6 Air kerma area product (KAP)

The patient skin dose is increasing as the KAP increases as in figures 4.7. The result shows the correlation between KAP and patient dose with good correlation of 0.8.

5.1.3.7 The fluoroscopic time

The patient skin dose is increasing as the fluoroscopic time increases as in figures 4.8 showed the fluoroscopic time and the correlation with the patient skin dose. The mean fluoroscopic time was 305 ± 272 second with the range of 13- 926 second. The correlation between patient skin dose and fluoroscopic time is $r = 0.7$.

5.1.3.8 The number of frames

The range of frames was 2-5, the range of skin dose was 0.1-0.7 Gy. Figure 4.9 showed the correlation between the number of frames and patient was poor as $r = 0.2$.

5.1.4 The patient skin dose determined by MIDSOF and System FPD

MIDSOF is useful for measuring skin radiation in real time. However, the measurement of the skin dose is at only a single point on the surface for its small size of detector. Therefore, to be effective, the detector of MIDSOF must be placed in the field of maximum X-ray exposure; however, it is impossible to predict the site of maximum X-ray exposure before intervention procedure commences.

As MIDSOF dosimeter is easily use and there was no need to estimate the surface area expose as in KAP method, KAP meter shows all exposures readout, some exposure is sometime not at the target organ.

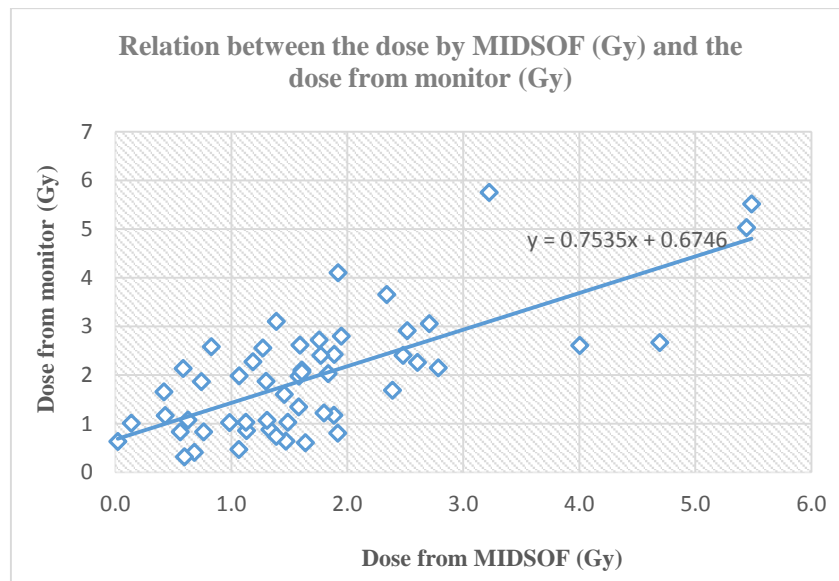
The x-ray tube moves during the procedure resulting in the inaccuracy of the exposed area as well as inaccuracy of the average skin dose. However, MIDSOF detector could identify the result in limited and fix area because of the small size of detector.

When we compare the MIDSOF readout with the system detector, the mean and range were $1.71+1.14(0.02-5.48)$ and $1.96+1.21(0.33-5.76)$. The percent difference between both readouts was 12.75. MIDSOF readout was lower than the monitor as the detector size is smaller.

5.1.5 The relationship between KAP method and MIDSOF.

The result shows the correlation between the estimated dose from KAP meter and the skin dose from MIDSOF with $r = 0.76$. As the KAP is the cumulative dose from every exposure to parts of the patient, so the dose could be estimated from the average radiation areas, while MIDSOF measured on real exposed skin.

5.1.6 The relationship between dose from MIDSOF and dose from monitor.



The result shows the correlation between the estimated dose from monitor and the skin dose from MIDSOF with $r = 0.7$.

5.1.7 The effective dose

In this study, the effective dose was calculated by using conversion coefficient 0.015 mSv/mGy.cm for CT multiplies DLP value (mGy.cm) [15]. The effective dose was calculated by using conversion coefficient 0.26 mSv/Gy.cm^2 for fluoroscopic multiplied KAP (Gy.cm^2) [16].

5.1.7.1 Patient effective dose from fluoroscopic examination

Sixty-two patients who underwent intervention procedures consists of 54 cases for TACE and 8 cases for PTBD. The mean+SD (range) of the effective dose of fluoroscopic system of TACE was $70.86 (15.57-188.55) \text{ mSv}$. The mean+SD of the effective dose of PTBD was $5.69 \pm 7.01 (0.43- 22.6) \text{ mSv}$. KAP readout was the major factors affecting effective dose.

5.1.7.2 Patient effective dose from CT examination

The mean \pm SD of the effective dose from CT of TACE was 6.93 (3.19 - 20.47) mSv. The key factors that affecting to high dose in CT were scan length, tube voltage and mAs.

The mean effective dose and range was 83.12 (19.88 – 357.8) mSv. The effective dose for fluoroscopic of TACE was approximately 10 times of the CT.

5.2 Conclusion

TACE procedure

The mean KAP was 379.88 Gy cm^2 , the fluoroscopic time was 33 min.

The mean patient skin dose determined by MIDSOF was 1.71 Gy.

The mean effective dose of fluoroscopic system was 70.86 mSv.

PTBD procedure

The mean KAP was 21.9 Gy cm^2 .

The mean effective dose was 5.69 mSv.

The mean patient dose was 0.14 Gy.

Factors affecting radiation dose

Good relation between skin dose and

- Air kerma area product (KAP)
- fluoroscopic time

Weak relation between skin dose and

- patient characteristics
- experience of radiologist
- The number of frames

Summary

The patient skin dose is very important during the intervention procedures. Radiologist and staff should be aware of several parameters influencing dose, therefore the case record form should be conducted. In case of over exposure leading to skin injury, the radiologist should inform the clinician to follow up for such the late effects. Both patient and staff are at risk of radiation injury, appropriate equipment and training are needed to minimize the risk.

Recommendations

The correlation factor should be posted for the staff awareness such as fluoroscopic time by keep beam-on time to a minimum, keep tube current (mAs) as low as possible and tube potential (kVp) as high as applicable, keep x-ray tube at maximum and the FPD at minimum distance from patient .



REFERENCES

1. Saenchon, P., The determination of average patient skin dose and its factors affecting in cardiac catheterization procedures. Thesis (M.Sc) Chulalongkorn University. , 2006.
2. Mahesh, M., Patient radiation exposure issues. . RadioGraphics. , Jul-Aug2001. 1033-45.
3. Shrimpton PC, W.B., Jones DG, Fisher ES. , The measurement of energy imparted to patients during diagnostic x-ray examinations using the Diamentor exposure-area product meter. Physics in Medicine and Biology. , 1984. 29(10):1199.
4. Ishikawa, M., Development of a wavelength-separated type scintillator with optical fiber (SOF) dosimeter to compensate for the cerenkov radiation effect. Journal of Radiation Research, 2015. 56: p. 372-381.
5. Htye N, J.J., Diagnostic Cerebral and Peripheral Angiography. . 2014: p. 1-55.
6. Nickoloff, E., Survey of Modern Fluoroscopy Imaging: Flat-Panel Detectors versus Image Intensifiers and More. RadioGraphics., 2011. 31: p. 591-602.
7. Dendy, P.H., B Physics for diagnostic radiology Philadelphia: Institute of Physics publication, 1990: p. 145.
8. Kalender, W., X-ray computed tomography. Physics in Medicine and Biology., 2006. 51(13)R29-43.
9. ACR–ASNR, Practice guideline for the performance and interpretation of Cervicocerebral computed tomography angiography (CTA). Available from <http://www.asnr.org/sites/default/files/guidelines/CervicocerebralAngio.pdf>.
10. Martin, C., Effective dose: how should it be applied to medical exposures. The British journal of radiology, 2007. 80(956):639-47.
11. Sitthiphan, P., The determination of patient effective dose in transarterial oily chemoembolization (TOCE) procedure using digital flat–panel system. . Master Degree, Thesis (M.Sc) Chulalongkorn University., 2009.
12. Kumkrue, C., Patient skin dose measurement in cardiac catheterization and interventional radiology. Master Degree, Thesis (M.Sc) Chulalongkorn University., 2004.
13. American Association of Physicist in Medicine. Specification and acceptance testing of computed tomography scanners, report 39 (May 1993).

14. American Association of Physicists in Medicine REPORT NO. 96, 2008(13).
15. Ionizing Radiation Exposure of the Population of the United States National Council on Radiation Protection and Measurements (NCRP) Report No. 160 [https://rpop.iaea.org/RPOP/RPoP/Content/InformationFor/HealthProfessionals/4_InterventionalRadiology/patient-staff-dose fluoroscopy.htm](https://rpop.iaea.org/RPOP/RPoP/Content/InformationFor/HealthProfessionals/4_InterventionalRadiology/patient-staff-dose%20fluoroscopy.htm), 2009.
16. Sapiin, B.K., Ng. Abdulah, BJJ, Radiation dose to patients Underdoing Interventional Radiological Procedure in Selected Hospitals in Malaysia: Retrospective Study. J HK coll Radiol 7 2004: p. 129-136.
17. BOR, D., Comparison effective dose obtained from dose-area product and air kerma measurement in interventional radiology. The British Journal of radiology 77, 2004: p. 315-322.
18. Shigeru Suzuki, S.F., Ikuo Kobayashi Yamauchi, et al Radiation Dose in patients and Radiologists During Transcatherter Arterial Embolization:Comparison of a Digital Flat-panel system and Conventional Unit. American Journal of Roentgenology 185, 2005: p. 855-859.
19. Eliseo Vano, R.S., J. M. Fernandez, J. J. Gallego, J. F. Verdu and M. Gonzalez de Garray. , Patient Dose Reference Levels for Interventional Radiology. A National Approach. Cardiovasc Intervent Radiol 32 2009: p. 19-24.
20. E. Papageorgiou E, V.T., I. A. Tsalafoutas, E. Maurikou, et al, Comparision of patient dose in interventional radiology procedures performed in two large hospital in Greece. Radiation Protection Dosimetry 124 2007: p. 97-102.
21. Svetlana Sarycheva, V.G.a.S.K., Studies of patient dose in interventional radiological examinations. Radiation Protection Dosimetry, 2010: p. 97-102.



APPENDIX

จุฬาลงกรณ์มหาวิทยาลัย
CHULALONGKORN UNIVERSITY

APPENDIX A

Case Record Form

Table I: Clinical data collection sheet for TACE procedure

Clinical data collection sheet for TACE procedure in interventional radiology unit	
Facility identification	
Equipment ID	
Initial KAP setting	
Initial cumulative fluoroscopy time	
Date	
Patient Study Number	
Height	
Weight	
Gender	
Age	
MIDSOF in place	
start time	
Fluoroscopy mode	
End time	
KAP readout at end	
Cumulative fluoroscopy time at end	
Number of frames	
Frame rate	
kVp	
mAs	
FOV	
Filter	
Dose from MIDSOF	

Table II: Clinical data collection sheet for PTBD procedure

Clinical data collection sheet for PTBD procedure in interventional radiology unit	
Facility identification	
Equipment ID	
Initial KAP setting	
Initial cumulative fluoroscopy time	
Date	
Patient Study Number	
Height	
Weight	
Gender	
Age	
MIDSOF in place	
start time	
Fluoroscopy mode	
End time	
KAP readout at end	
Cumulative fluoroscopy time at end	
Number of frames	
Frame rate	
kVp	
mAs	
FOV	
Filter	
Dose from MIDSOF	

Table III: Clinical data collection sheet for CT procedure

Date	
Patient study number	
Gender (M/F)	
Age (year)	
Height (cm)	
Weight (kg)	
kVp	
Total mAs	
Total DLP (mGycm)	
Skin dose from MIDSOF	

Table IV: Complexity index of TACE procedure

Patient Study Number	
Date (D/M/Y) Gender (M/F) Age (years) Height (cm.) Weight (kg) Disease TACE No Procedure Elective/Emergency	
No. of tumor	<input type="radio"/> single <input type="radio"/> 2 or 3 <input type="radio"/> multiple
Location	<input type="radio"/> Right <input type="radio"/> Left <input type="radio"/> Both lobes
Hepatic segment(s) segment 1 to 8	
Maximum tumor diameter (cm.)	
Branching 0 : no side branch 1 : bifurcation 2 : trifurcation	
Embolic material Anticancer drug Complication during procedure	
Operators experience in interventional Radiologist Assistant	
Complexity index	<input type="radio"/> Easy <input type="radio"/> Moderate <input type="radio"/> Difficult <input type="radio"/> Extremely Difficult

APPENDIX B

Patient Information Sheet

เอกสารข้อมูลคำอธิบายสำหรับผู้ป่วยที่เข้าร่วมการวิจัย

ชื่อโครงการวิจัย การวัดปริมาณรังสีของผู้ป่วยในการตรวจรักษาตับ โดยวิธีทีเอซี อี (TACE) และการตรวจรักษาทางเดินน้ำดีโดยวิธีพีทีบีดี (PTBD) โดยใช้เครื่อง มิคซอฟ ในการตรวจวัด

ผู้วิจัยหลัก

ชื่อ นางสาวสายวรุณ เทียนเครือ
 ที่อยู่ทำงานหรือสถานศึกษาของผู้วิจัย ภาควิชารังสีวิทยา คณะแพทยศาสตร์ 1873
 ถนนพระราม 4 ปทุมวัน กรุงเทพมหานคร
 10330
 เบอร์โทรศัพท์ติดต่อ 24 ชั่วโมง 085-1803091

ผู้วิจัยร่วม

ชื่อ รองศาสตราจารย์ดร. อัญชดี กฤษณจิตา
 ที่อยู่ทำงานหรือสถานศึกษาของผู้วิจัย ภาควิชารังสีวิทยา คณะแพทยศาสตร์ 1873
 ถนนพระราม 4 ปทุมวัน กรุงเทพมหานคร
 10330
 เบอร์โทรศัพท์ 081-6305890

แหล่งทุน ไม่มี

เรียน ผู้เข้าร่วมโครงการวิจัยทุกท่าน

ท่านได้รับเชิญให้เข้าร่วมในโครงการวิจัยนี้เนื่องจากท่านเป็นผู้ป่วยที่ได้รับการตรวจรักษา โดยวิธีทีเอซีอี (TACE) และการตรวจรักษาทางเดินน้ำดีโดยวิธีพีทีบีดี (PTBD) ก่อนที่ท่านจะตัดสินใจเข้าร่วมในการศึกษาวิจัยดังกล่าว ขอให้ท่านอ่านเอกสารฉบับนี้อย่างถี่ถ้วน เพื่อให้ท่านได้ทราบถึงเหตุผลและรายละเอียดของการศึกษาวิจัยในครั้งนี้ หากท่านมีข้อสงสัยใดๆ เพิ่มเติม กรุณาซักถามจากผู้ทำวิจัย ซึ่งจะเป็นผู้สามารถตอบคำถามและให้ความกระจ่างแก่ท่านได้

ท่านสามารถขอคำแนะนำในการเข้าร่วมโครงการวิจัยนี้จากครอบครัว เพื่อน หรือแพทย์ประจำตัวของท่านได้ ท่านมีเวลาอย่างเพียงพอในการตัดสินใจโดยอิสระ ถ้าท่านตัดสินใจแล้วว่าจะเข้าร่วมในโครงการวิจัยนี้ ขอให้ท่านลงนามในเอกสารแสดงความยินยอมของโครงการวิจัยนี้

เหตุผลความเป็นมา

ผู้ป่วยที่เข้ารับการตรวจรักษาตับ โดยวิธีทีเอซีอี (TACE) และ การตรวจรักษาทางเดินน้ำดี โดยวิธีพีทีบีดี (PTBD) ซึ่งเป็นการตรวจทางด้านรังสีร่วมรักษาโดยใช้รังสีแบบต่อเนื่อง (Fluoroscopy) นั้น จะมีความเสี่ยงที่จะได้รับปริมาณรังสีสูงกว่า การตรวจวินิจฉัยอื่นๆ และ ปริมาณที่ได้รับจะอยู่ในระดับเกณฑ์ที่สามารถยอมรับได้หรือไม่เป็นสิ่งที่น่าศึกษาอย่างยิ่ง

วัตถุประสงค์ของการศึกษา

วัตถุประสงค์หลักจากการศึกษาในครั้งนี้คือวัดปริมาณรังสีที่ผิวหนังของผู้ป่วยต่อการตรวจหรือรักษาแต่ละครั้งว่ามีปริมาณเท่าไร เพื่อไม่ให้เกินปริมาณรังสีสูงสุดที่ผู้ป่วยสามารถรับได้และมีวิธีการลดปริมาณรังสีผู้ป่วยได้รับอย่างไรในการตรวจแต่ละครั้ง เพื่อศึกษาพารามิเตอร์ที่มีผลต่อปริมาณรังสีที่ผิวหนังของผู้ป่วยได้รับจากการตรวจรักษาตับโดยวิธีทีเอซีอี (TACE) และการตรวจรักษาทางเดินน้ำดีโดยวิธีพีทีบีดี (PTBD) โดยใช้เครื่องมือคซอพ (MIDSOF) ที่เป็นซินทิลเลเตอร์และ แดพมิเตอร์

วิธีการที่เกี่ยวข้องกับการวิจัย

หลังจากท่านให้ความยินยอมที่จะเข้าร่วมในโครงการวิจัยนี้ ผู้วิจัยจะขอเก็บข้อมูลในการวัดปริมาณรังสีนั้นจะใช้เครื่องวัดรังสีชนิดที่เป็นซินทิลเลเตอร์ คซอพ (MIDSOF) ซึ่งมีขนาดของ

หัววัด 1 มม. มีสายต่อเข้าเครื่องอ่านโดยตรงและสามารถอ่านค่าได้ทันที ในการวัดโดยใช้เครื่องวัดมิดซอพ (MIDSOF) นั้นจะใช้หัววัดรังสีติดที่ตำแหน่งด้านหลังของผู้ป่วยให้ตรงกับตำแหน่งตรงกลางตับ สำหรับการวัดโดยใช้แคปมิเตอร์ (KAP meter) ซึ่งเป็นเครื่องมือที่ใช้วัดปริมาณรังสีที่ออกจากหลอดเอกซเรย์โดยตรง

ส่วนหัววัดจะติดอยู่ที่หลอดเอกซเรย์โดยเครื่องอ่านค่าจะแยกออกมาต่างหาก ซึ่งอุปกรณ์ทั้ง 2 ชนิดนี้จะไม่รบกวนหรือเป็นอุปสรรค ทั้งผู้ป่วยและเจ้าหน้าที่ในขณะที่ปฏิบัติงาน

ประชากรที่ศึกษา : การศึกษานี้เป็นการศึกษาในผู้ป่วยที่เข้ารับการตรวจรักษาด้วยวิธีที่เอซีอี TACE (Transarterial Chemoembolization) จำนวน 52 คน และตรวจรักษาทางเดินน้ำดีโดยวิธีพีทีบีดี PTBD (Percutaneous Transhepatic Biliary Drainage) จำนวน 10 คน ที่โรงพยาบาลจุฬาลงกรณ์ สภากาชาดไทย ตั้งแต่เดือนกรกฎาคม ปีพ.ศ. 2559 โดยผู้ป่วยจะต้องอายุไม่น้อยกว่า 18 ปีบริบูรณ์และต้องรู้สีกตัว

ความรับผิดชอบของอาสาสมัครผู้เข้าร่วมในโครงการวิจัย

เพื่อให้งานวิจัยนี้ประสบความสำเร็จ ผู้ทำวิจัยใคร่ขอความความร่วมมือจากท่าน โดยจะขอให้ท่านปฏิบัติตามคำแนะนำของผู้ทำวิจัย รวมทั้งแจ้งอาการผิดปกติต่าง ๆ ที่เกิดขึ้นกับท่านระหว่างที่ท่านเข้าร่วมในโครงการวิจัยให้ผู้ทำวิจัยได้รับทราบ

ความเสี่ยงที่อาจได้รับ

ท่านอาจเกิดการระคายเคืองจากเครื่องมือและอุปกรณ์ที่ใช้ในการติดบริเวณแผ่นหลังเพื่อตรวจวัดรังสีเพียงเล็กน้อย กรุณาแจ้งผู้ทำวิจัยในกรณีที่พบอาการดังกล่าวข้างต้น หรืออาการอื่น ๆ ที่พบร่วมด้วย ระหว่างที่อยู่ในโครงการวิจัย

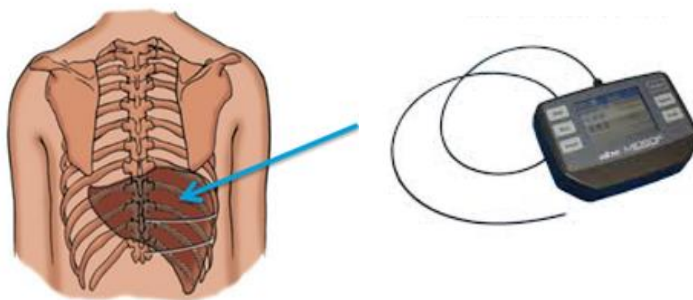
ประโยชน์ที่อาจได้รับ

ผู้ป่วยสามารถทราบปริมาณรังสีที่ผิวหนังที่ผู้ป่วยได้รับในการตรวจครั้งนี้ หลังจากที่แพทย์และเจ้าหน้าที่ที่ทำการตรวจหรือรักษาเสร็จในแต่ละการตรวจ ผู้วิจัยจะทำการเก็บและอ่านข้อมูลของเครื่องมือวัดและนำค่าที่ได้จากแคปมิเตอร์และเครื่องมือมิดซอพมาทำการคำนวณหาปริมาณรังสีที่ผู้ป่วยได้รับในการตรวจครั้งนั้นๆ

ข้อปฏิบัติของท่านขณะที่ร่วมในโครงการวิจัย

จะมีข้อมูลและข้อปฏิบัติร่วมกันดังนี้

1. ในการทำการวิจัยในครั้งนี้จะทำการวิจัยในอาสาสมัคร 62 คน
2. ท่านไม่ต้องเสียค่าใช้จ่ายใดๆ เพื่อการวัดค่าปริมาณรังสีดังกล่าว
3. ก่อนเริ่มตรวจในแต่ละครั้ง ผู้วิจัยจะติดเครื่องมือคือ เครื่องตรวจมิตซอพ บริเวณหลังผู้ป่วย 1 จุด
4. ท่านอาจเกิดการระคายเคืองจากเครื่องมือและอุปกรณ์ที่ใช้ในการติดบริเวณแผ่นหลังเพื่อตรวจวัดรังสีเพียงเล็กน้อย
5. หากเกิดอันตรายใดๆ จากการวิจัยดังกล่าว ผู้วิจัยจะได้รับการพยาบาลโดยไม่เสียค่าใช้จ่าย
6. หลังจากที่แพทย์และเจ้าหน้าที่ทำการตรวจหรือรักษาเสร็จในแต่ละการตรวจ ผู้วิจัยจะทำการเก็บและอ่านข้อมูลของเครื่องมือวัดและนำค่าที่ได้จากแคปมิเตอร์และเครื่องมือมิตซอพ มาทำการคำนวณหาปริมาณรังสีที่ผู้ป่วยได้รับในการตรวจครั้งนั้นๆ
7. การเข้าร่วมการศึกษาวิจัยครั้งนี้ เป็นไปโดยสมัครใจ ท่านอาจปฏิเสธที่จะเข้าร่วมการวิจัย หรือถอนตัวจากการวิจัยนี้ได้ทุกเมื่อโดยไม่จำเป็นต้องแจ้งเหตุผล
8. ผู้วิจัยรับรองว่าจะเก็บข้อมูลเฉพาะเกี่ยวกับตัวผู้เข้าร่วมวิจัยเป็นความลับ โดยจะไม่มีเปิดเผยชื่อของท่านตามกฎหมาย และจะเปิดเผยได้เมื่อได้รับการยินยอมจากผู้เข้าร่วมการวิจัยเท่านั้น บุคคลอื่นในนามของผู้สนับสนุนการวิจัย คณะกรรมการพิจารณาจริยธรรมการวิจัย ในคน อาจจะได้รับอนุญาตให้เข้ามาตรวจและประมวลข้อมูลส่วนตัวของผู้เข้าร่วมวิจัย ทั้งนี้ จะต้องกระทำไปเพื่อตรวจสอบความถูกต้องของข้อมูลเท่านั้นและจะต้องได้รับคำยินยอมที่จะให้มีการตรวจสอบข้อมูลจากผู้เข้าร่วมวิจัยเท่านั้น



ระยะเวลาที่อาสาสมัครแต่ละคนต้องอยู่ในโครงการ (Duration of participation for each volunteer)

เวลาที่ผู้ป่วยได้รับการตรวจรักษาตับโดยวิธีทีเอซีอี TACE และการตรวจรักษาทางเดินน้ำดีโดยวิธีพีทีบีดี PTBD ทางด้านรังสีร่วมรักษาโดยการใช้รังสีแบบต่อเนื่อง (Fluoroscopy) 2-3 ชั่วโมง

อันตรายที่อาจเกิดขึ้นจากการเข้าร่วมในโครงการวิจัยและความรับผิดชอบของผู้ทำวิจัย

หากพบอันตรายที่เกิดขึ้นจากการเข้าร่วมการวิจัย ท่านจะได้รับการรักษาอย่างเหมาะสมทันที หากท่านปฏิบัติตามคำแนะนำของทีมผู้ทำวิจัยแล้ว ผู้ทำวิจัยยินดีจะรับผิดชอบค่าใช้จ่ายในการรักษาพยาบาลของท่าน

ในกรณีที่ท่านได้รับอันตรายใด ๆ หรือต้องการข้อมูลเพิ่มเติมที่เกี่ยวข้องกับโครงการวิจัย ท่านสามารถติดต่อกับผู้ทำวิจัยคือ นางสาวสายวรุณ เทียนเครือ 085-1803091 ซึ่งยินดีให้คำตอบแก่ท่านทุกเมื่อได้ตลอด 24 ชั่วโมง

ค่าใช้จ่ายของท่านในการเข้าร่วมการวิจัย

ท่านไม่ต้องเสียค่าใช้จ่ายใดๆ เพื่อการวัดค่าปริมาณรังสีดังกล่าว

ค่าตอบแทนสำหรับผู้เข้าร่วมวิจัย

ท่านจะไม่ได้รับเงินค่าตอบแทนจากการเข้าร่วมในการวิจัยครั้งนี้ ท่านจะไม่ได้รับเงินค่าตอบแทนในเรื่องค่าชดเชย ค่าเดินทาง ค่าเสียเวลา ความไม่สะดวกสบาย

การเข้าร่วมและการสิ้นสุดการเข้าร่วมโครงการวิจัย

การเข้าร่วมในโครงการวิจัยครั้งนี้เป็นไปโดยความสมัครใจ หากท่านไม่สมัครใจจะเข้าร่วมการศึกษาแล้ว ท่านสามารถถอนตัวได้ตลอดเวลา การขอถอนตัวออกจากโครงการวิจัยโดยไม่จำเป็นต้องแจ้งเหตุผล การขอถอนตัวออกจากโครงการวิจัยจะไม่มีผลต่อการดูแลรักษาโรคของท่านแต่อย่างใด อาสาสมัครสามารถส่งบันทึกขอยกเลิกความยินยอมทางไปรษณีย์ได้ที่นางสาวสายวรุณ เทียนเครือ ที่อยู่หรือสถานศึกษาของผู้วิจัย ภาควิชารังสีวิทยา คณะแพทยศาสตร์ 1873 ถนนพระราม 4 ปทุมวัน กรุงเทพมหานคร 10330

การปกป้องรักษาข้อมูลความลับของอาสาสมัคร

ข้อมูลนี้อาจนำไปสู่การเปิดเผยตัวท่าน จะได้รับการปกปิดและจะไม่เปิดเผยแก่สาธารณชน ในกรณีที่ผลการวิจัยได้รับการตีพิมพ์ ชื่อและที่อยู่ของท่านจะต้องได้รับการปกปิดอยู่เสมอ โดยจะใช้เฉพาะรหัสประจำโครงการวิจัยของท่าน

จากการลงนามยินยอมของท่าน ผู้ทำวิจัย คณะกรรมการจริยธรรมการวิจัย ผู้ตรวจสอบการวิจัย และหน่วยงานควบคุมระเบียบกฎหมาย สามารถเข้าไปตรวจสอบบันทึกข้อมูลทางการแพทย์ของท่านได้แม้จะสิ้นสุดโครงการวิจัยแล้วก็ตาม โดยไม่ละเมิดสิทธิของท่านในการรักษาความลับเกินขอบเขตที่กฎหมายและระเบียบกฎหมายอนุญาตไว้

สิทธิของผู้เข้าร่วมในโครงการวิจัย

ในฐานะที่ท่านเป็นผู้เข้าร่วมในโครงการวิจัย ท่านจะมีสิทธิ์ดังต่อไปนี้

1. ท่านจะได้รับทราบถึงลักษณะและวัตถุประสงค์ของการวิจัยในครั้งนี้
2. ท่านจะได้รับการอธิบายเกี่ยวกับระเบียบวิธีการของการวิจัย รวมทั้งอุปกรณ์ที่ใช้ในการวิจัยครั้งนี้
3. ท่านจะได้รับการอธิบายถึงความเสี่ยงและความไม่สบายที่จะได้รับการวิจัย
4. ท่านจะได้รับการอธิบายถึงประโยชน์ที่ท่านอาจจะได้รับการวิจัย
5. ท่านจะมีโอกาสได้ซักถามเกี่ยวกับงานวิจัยหรือขั้นตอนที่เกี่ยวข้องกับงานวิจัย
6. ท่านจะได้รับทราบว่ากรยินยอมเข้าร่วมในโครงการวิจัยนี้ ท่านสามารถขอถอนตัวจากโครงการเมื่อไรก็ได้ โดยผู้เข้าร่วมในโครงการวิจัยสามารถขอถอนตัวจากโครงการโดยไม่ได้รับผลกระทบใด ๆ ทั้งสิ้น
7. ท่านจะได้รับเอกสารข้อมูลคำอธิบายสำหรับผู้เข้าร่วมในโครงการวิจัยและสำเนาเอกสารใบยินยอมที่มีทั้งลายเซ็นและวันที่
8. ท่านมีสิทธิ์ในการตัดสินใจว่าจะเข้าร่วมในโครงการวิจัยหรือไม่ก็ได้ โดยปราศจากการใช้อิทธิพลบังคับข่มขู่ หรือการหลอกลวง

หากท่านไม่ได้รับการชดเชยอันควรต่อการบาดเจ็บหรือเจ็บป่วยที่เกิดขึ้นโดยตรงจากการวิจัย หรือท่านไม่ได้รับการปฏิบัติตามที่ปรากฏในเอกสารข้อมูลคำอธิบายสำหรับผู้เข้าร่วมในการวิจัย ท่านสามารถร้องเรียนได้ที่ สำนักงานคณะกรรมการจริยธรรมการวิจัย คณะแพทยศาสตร์ จุฬาลงกรณ์มหาวิทยาลัย ตึกอำนวยการ ชั้น 3 โรงพยาบาลจุฬาลงกรณ์ ถนนพระราม 4 ปทุมวัน กรุงเทพฯ 10330 โทร 0-2256-4493 ในเวลาราชการ

การลงนามในเอกสารให้ความยินยอม ไม่ได้หมายความว่าท่านได้สละสิทธิ์ทางกฎหมายตามปกติที่ท่านพึงมี ขอขอบคุณในการให้ความร่วมมือของท่านมา ณ ที่นี้



APPENDIX C

Consent form

ใบยินยอมเข้าร่วมการวิจัย

การวิจัย เรื่อง การวัดปริมาณรังสีของผู้ป่วยในการตรวจรักษาตับ โดยวิธีทีเอซีอี (TACE) และการตรวจรักษาทางเดินน้ำดี โดยวิธีพีทีบีดี (PTBD) โดยใช้เครื่อง มิตรซอฟ ในการตรวจวัด

วันที่คำยินยอม วันที่.....เดือน.....พ.ศ.....

ข้าพเจ้า นาย/นาง/นางสาว.....

ที่อยู่.....

ได้อ่านรายละเอียดจากเอกสารข้อมูลสำหรับผู้เข้าร่วมโครงการวิจัยวิจัยที่แนบมาฉบับวันที่..... และข้าพเจ้ายินยอมเข้าร่วมโครงการวิจัยโดยสมัครใจ

ข้าพเจ้าได้รับสำเนาเอกสารแสดงความยินยอมเข้าร่วมในโครงการวิจัยที่ข้าพเจ้าได้ลงนาม และ วันที่ พร้อมด้วยเอกสารข้อมูลสำหรับผู้เข้าร่วมโครงการวิจัย ทั้งนี้ก่อนที่จะลงนามในใบยินยอมให้ทำการวิจัยนี้ ข้าพเจ้าได้รับการอธิบายจากผู้วิจัยถึงวัตถุประสงค์ของการวิจัย ระยะเวลาของการทำวิจัย วิธีการวิจัย อันตราย หรืออาการที่อาจเกิดขึ้นจากการวิจัย หรือจากยาที่ใช้ รวมทั้งประโยชน์ที่จะเกิดขึ้นจากการวิจัย และแนวทางการรักษาโดยวิธีอื่นอย่างละเอียด ข้าพเจ้ามีเวลาและโอกาสเพียงพอในการซักถามข้อสงสัยจนมีความเข้าใจอย่างดีแล้ว โดยผู้วิจัยได้ตอบคำถามต่าง ๆ ด้วยความเต็มใจไม่ปิดบังซ่อนเร้นจนข้าพเจ้าพอใจ

ข้าพเจ้ารับทราบจากผู้วิจัยว่าหากเกิดอันตรายใด ๆ จากการวิจัยดังกล่าว ข้าพเจ้าจะได้รับการรักษาพยาบาลโดยไม่เสียค่าใช้จ่าย

ข้าพเจ้ามีสิทธิที่จะบอกเลิกเข้าร่วมในโครงการวิจัยเมื่อใดก็ได้ โดยไม่จำเป็นต้องแจ้งเหตุผล และการบอกเลิกการเข้าร่วมการวิจัยนี้ จะไม่มีผลต่อการรักษาโรคหรือสิทธิอื่น ๆ ที่ข้าพเจ้าจะพึงได้รับต่อไป

ผู้วิจัยรับรองว่าจะเก็บข้อมูลส่วนตัวของข้าพเจ้าเป็นความลับ และจะเปิดเผยได้เฉพาะเมื่อได้รับการยินยอมจากข้าพเจ้าเท่านั้น คณะกรรมการพิจารณาจริยธรรมการวิจัยในคนอาจได้รับอนุญาตให้เข้ามาตรวจและประมวลข้อมูลของ

ข้าพเจ้า ทั้งนี้จะต้องกระทำไปเพื่อวัตถุประสงค์เพื่อตรวจสอบความถูกต้องของข้อมูลเท่านั้น โดยการตกลงที่จะเข้าร่วมการศึกษานี้ข้าพเจ้าได้ให้คำยินยอมที่จะให้มีการตรวจสอบข้อมูลประวัติทางการแพทย์ของข้าพเจ้าได้

ผู้วิจัยรับรองว่าจะไม่มีการเก็บข้อมูลใด ๆ เพิ่มเติม หลังจากที่ข้าพเจ้าขอยกเลิกการเข้าร่วมโครงการวิจัยและต้องการให้ทำลายเอกสารและ/หรือ ตัวอย่างที่ใช้ตรวจสอบทั้งหมดที่สามารถสืบค้นถึงตัวข้าพเจ้าได้

ข้าพเจ้าเข้าใจว่า ข้าพเจ้ามีสิทธิ์ที่จะตรวจสอบหรือแก้ไขข้อมูลส่วนตัวของข้าพเจ้าและสามารถยกเลิกการให้สิทธิในการใช้ข้อมูลส่วนตัวของข้าพเจ้าได้ โดยต้องแจ้งให้ผู้วิจัยรับทราบ

ข้าพเจ้าได้ตระหนักว่าข้อมูลในการวิจัยรวมถึงข้อมูลทางการแพทย์ของข้าพเจ้าที่ไม่มีการเปิดเผยชื่อ จะผ่านกระบวนการต่าง ๆ เช่น การเก็บข้อมูล การบันทึกข้อมูลในระบบบันทึกและในคอมพิวเตอร์ การตรวจสอบ การวิเคราะห์ และการรายงานข้อมูลเพื่อวัตถุประสงค์ทางวิชาการรวมทั้งการใช้ข้อมูลทางการแพทย์ในอนาคตหรือการวิจัยทางด้านเภสัชภัณฑ์ เท่านั้น

ข้าพเจ้าได้อ่านข้อความข้างต้นและมีความเข้าใจดีทุกประการแล้ว ยินดีเข้าร่วมในการวิจัยด้วยความเต็มใจ จึงได้ลงนามในเอกสารแสดงความยินยอมนี้

.....ลงนามผู้ให้ความยินยอม
(.....) ชื่อผู้ยินยอมตัวบรรจง
วันที่เดือน.....พ.ศ.....

ข้าพเจ้าได้อธิบายถึงวัตถุประสงค์ของการวิจัย วิธีการวิจัย อันตราย หรืออาการไม่พึงประสงค์หรือความเสี่ยงที่อาจเกิดขึ้นจากการวิจัย หรือจากยาที่ใช้ รวมทั้งประโยชน์ที่จะเกิดขึ้นจากการวิจัยอย่างละเอียด ให้ผู้เข้าร่วมในโครงการวิจัยตามนามข้างต้น ได้ทราบและมีความเข้าใจดีแล้ว พร้อมลงนามลงในเอกสารแสดงความยินยอมด้วยความเต็มใจ

.....ลงนามผู้ทำวิจัย
(.....) ชื่อผู้ทำวิจัย ตัวบรรจง
วันที่เดือน.....พ.ศ.....

.....ลงนามพยาน
(.....) ชื่อพยาน ตัวบรรจง
วันที่เดือน.....พ.ศ.....

Complexity Index

Patient Study Number	11	12	13	14	15	16	17	18	19	20
Date (DDMMY)	22/7/2559	22/7/2559	25/7/2559	25/7/2559	28/7/2559	28/7/2559	27/7/2559	27/7/2559	28/7/2559	28/7/2559
Gender (M/F)	F	M	M	M	M	M	F	M	M	M
Age (years)	92	64	60	60	56	53	87	46	86	60
Height (cm.)	148	167	165	175	164	170	151	170	170	160
Weight (kg)	45.6	63.5	65.9	59	46.5	65	56	74	66	53
Disease	HCC									
TACE No	2	1	3	7	2	1	1	1	1	4
Procedure (Elective/Emergency)	Elective									
No. of tumor	<ul style="list-style-type: none"> ● single ○ 2 or 3 ◐ multiple 	<ul style="list-style-type: none"> ● single ○ 2 or 3 ◐ multiple 	<ul style="list-style-type: none"> ● single ○ 2 or 3 ◐ multiple 	<ul style="list-style-type: none"> ● single ○ 2 or 3 ◐ multiple 	<ul style="list-style-type: none"> ● single ○ 2 or 3 ◐ multiple 	<ul style="list-style-type: none"> ● single ○ 2 or 3 ◐ multiple 	<ul style="list-style-type: none"> ● single ○ 2 or 3 ◐ multiple 	<ul style="list-style-type: none"> ● single ○ 2 or 3 ◐ multiple 	<ul style="list-style-type: none"> ● single ○ 2 or 3 ◐ multiple 	<ul style="list-style-type: none"> ● single ○ 2 or 3 ◐ multiple
Location	<ul style="list-style-type: none"> ● Right ○ Left ◐ Both lobes 	<ul style="list-style-type: none"> ● Right ○ Left ◐ Both lobes 	<ul style="list-style-type: none"> ● Right ○ Left ◐ Both lobes 	<ul style="list-style-type: none"> ● Right ○ Left ◐ Both lobes 	<ul style="list-style-type: none"> ● Right ○ Left ◐ Both lobes 	<ul style="list-style-type: none"> ● Right ○ Left ◐ Both lobes 	<ul style="list-style-type: none"> ● Right ○ Left ◐ Both lobes 	<ul style="list-style-type: none"> ● Right ○ Left ◐ Both lobes 	<ul style="list-style-type: none"> ● Right ○ Left ◐ Both lobes 	<ul style="list-style-type: none"> ● Right ○ Left ◐ Both lobes
Hepatic segment(s) segment 1 to 8	IV	VI	V	III, V	V, VI	V, VI	VII, VIII	VII, VIII	V, VIII	III, IIII
Maximum tumor diameter (cm.)	3.3*2.3	4.3	4.4	1.7	8.6, 9.1	4.6*3.2	3.4*2.9	1.9	8.1	8.7
Branching	1	1	1	1	1	1	1	2	2	2
0: no side branch										
1: bifurcation										
2: trifurcation										
Embolic material	Gelform									
Anticancer drug	MMC, 5-FU									
Complication during procedure										
Operator's experience in interventional										
Radiologist	Naicha, 5 years									
Assistant	Pongsakorn, 2 month									
Complexity Index	<ul style="list-style-type: none"> Easy √ Moderate Difficult Extremely Difficult 	<ul style="list-style-type: none"> Easy √ Moderate Difficult Extremely Difficult 	<ul style="list-style-type: none"> Easy √ Moderate Difficult Extremely Difficult 	<ul style="list-style-type: none"> √ Easy Moderate Difficult Extremely Difficult 	<ul style="list-style-type: none"> Easy √ Moderate Difficult Extremely Difficult 	<ul style="list-style-type: none"> Easy √ Moderate Difficult Extremely Difficult 	<ul style="list-style-type: none"> Easy √ Moderate Difficult Extremely Difficult 	<ul style="list-style-type: none"> Easy √ Moderate Difficult Extremely Difficult 	<ul style="list-style-type: none"> Easy √ Moderate Difficult Extremely Difficult 	<ul style="list-style-type: none"> Easy √ Moderate Difficult Extremely Difficult

Complexity Index

Patient Study Number	51	52	53	54
Date (D/M/Y)	6/2/2560	7/2/2560	14/2/2560	14/2/2560
Gender (M/F)	M	M	M	M
Age (years)	52	60	69	52
Height (cm.)	166	164	175	160
Weight (kg)	62.8	80	67	61
Disease	HCC	HCC	HCC	HCC
TACE No	6	2	1	2
Procedure Elective/Emergency				
No. of tumor	<input type="radio"/> single <input checked="" type="radio"/> 2 or 3 <input type="radio"/> multiple	<input checked="" type="radio"/> single <input type="radio"/> 2 or 3 <input type="radio"/> multiple	<input type="radio"/> single <input type="radio"/> 2 or 3 <input checked="" type="radio"/> multiple	<input checked="" type="radio"/> single <input type="radio"/> 2 or 3 <input type="radio"/> multiple
Location	<input checked="" type="radio"/> Right <input type="radio"/> Left <input type="radio"/> Both lobes	<input checked="" type="radio"/> Right <input type="radio"/> Left <input type="radio"/> Both lobes	<input type="radio"/> Right <input type="radio"/> Left <input checked="" type="radio"/> Both lobes	<input checked="" type="radio"/> Right <input type="radio"/> Left <input type="radio"/> Both lobes
Hepatic segment(s) segment 1 to 8	IV	IV	V	V
Maximum tumor diameter (cm.)	2.8*2.0	5.6	0.7	13.1*11.2
Branching	1	2	1	1
0: no side branch				
1: bifurcation				
2: trifurcation				
Embolic material	Gelform	Gelform	Gelform	Gelform
Anticancer drug	MMC,5-FU	MMC,5-FU	MMC,5-FU	MMC,5-FU
Complication during procedure				
Operators experience in interventional	Natcha, 5 years	Natcha, 5 years	Natcha, 5 years	Natcha, 5 years
Radiologist	Piya,4 month	Piya,4 month	Piya,4 month	Piya,4 month
Assistant				
Complexity index	Easy <input checked="" type="checkbox"/> Moderate <input type="checkbox"/> Difficult <input type="checkbox"/> Extremely Difficult	Easy <input checked="" type="checkbox"/> Moderate <input type="checkbox"/> Difficult <input type="checkbox"/> Extremely Difficult	Easy <input checked="" type="checkbox"/> Moderate <input type="checkbox"/> Difficult <input type="checkbox"/> Extremely Difficult	Easy <input checked="" type="checkbox"/> Moderate <input type="checkbox"/> Difficult <input type="checkbox"/> Extremely Difficult

APPENDIX E

Equipment performance for DSA system

Report of DSA system performance

Hospital	King Chulalongkorn Memorial Hospital
Room	DSA 1
Date	February 2017
X-ray unit	Toshiba IVR-CT
Test performed by	Saiwaroon Teankaeu


 Dose Assessment

Focus-Intensifier distance (cm) 100 cm.
 Patient dose measurement: Focus-Ionization chamber distance 60 cm.
 Entrance II dose measurement: II-Ionization chamber distance 40 cm.

Mode	Submode/ Image quality	Pulse rate (pulses/s)	Automatic added filtration (mm Cu)	Field size (inch)	kV	mA	(Patient entrance surface air kerma) (uGy/s)	Image Intensifier entrance air kerma (uGy/s)	Patient entrance surface air kerma at 60 cm (including backscatter (1.3)	phantom
Fluoro	DSA 3f/s	10	2.0	16.0	70.0	55.0	81.67	1.924	107.9	CIRS 930
Normal				12.0	70.0	66.0	105.200	2.468	139.0	
				8.0	70.0	92.0	171.400	2.7	226.5	
				6.0	70.0	113.0	228.4	2.3	301.9	

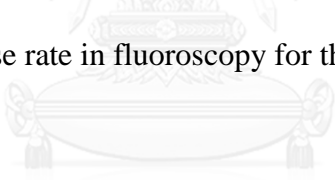
Automatic Brightness Control Test

Mode	Submode/ Image quality	Pulse rate (pulses/s)	Automatic added filtration (mm Cu)	Field size	added absorber (mm Cu)	kV	mA	Patient entrance surface air kerma (mR/min)
Normal	DSA 3f/s	10.0	2.0	16.0	CIRS	70	55	0.563
					add 1.5 mm Cu	88	198	6.115
					add 1.5 mm Cu + 1.5 mm lead	120	132	9.148
					add 1.5 mm Cu + 1.5 mm lead	120	132	18.740


 Table Attenuation

Mode	Submode/ Image quality	Dose rate (uGy/s)	Table attenuation (%)	Absorber
C-arm without table	Normal	585.8	7.1	1.5 mm Cu
C-arm with table	Normal	630.3		

Note: Measurement of dose rate in fluoroscopy for the same mode and field size



จุฬาลงกรณ์มหาวิทยาลัย
CHULALONGKORN UNIVERSITY

Half Value Layer Assessment

Al attenuator (mm)	Submode/ Image quality	Dose rate (uGy/s)	HVL (mm)
0.0	Normal	213	5.93 HVL = 6
2.0		163.3	
4.0		130.8	
6.0		105.7	

Note: Measurement of dose rate in fluoroscopy for the same mode and field size, add attenuator (copper sheets) on II. to drive kV to 70 kV

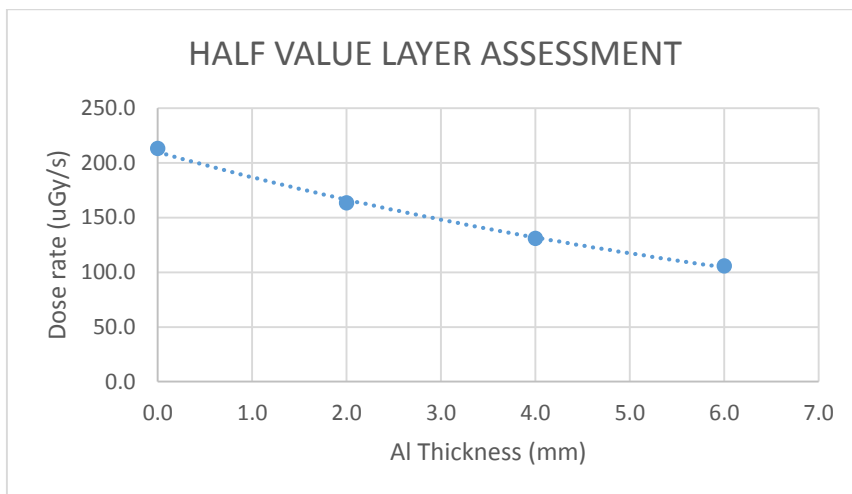


Image Quality Assessment

Resolution should be assessed in the usual illumination condition and from the operator’s position. Leeds Test placed on Image-Intensifier detector entrance surface with grid. All mode (fluoroscopy and image acquisition) and image qualities.

Focus-Image Intensifier distance 100 cm.

Mode	Submode/ Image quality	Automatic added filtration (mm Cu)	Field size (inch)	kV	mA	Live image			
						No. of ground	High contrast Resolution (lp/mm)	No. of disc	Low contrast (% contrast)
Normal	DSA 3 f/s	2.0	16.0	70.0	127.0	4.0	0.71	4.0	10.90
			12.0	70.0	137.0	5.0	0.8	4.0	10.90
			8.0	70.0	181.0	6.0	0.9	4.0	10.90
			6.0	72.0	200.0	7.0	1.0	4.0	10.90

APPENDIX E

Equipment performance for CT system

Position Dependence of CT Numbers

Method: Position the water phantom centered in the gantry. Using 8 cm slice thickness, obtain one scan using typical head technique. Select a circular region of interest of approximately 400 sq. mm. and then record the mean C.T. number and standard deviation for each of the positions 1 through 5.

Technique: 120 kVp, 200 mA, 1 sec, slice collimation 8 mm. 400 mm FOV.

Tolerance: The coefficient of variation of mean CT numbers of the four scans should be less than 0.2.

Results:

Position	Mean C.T.	S.D.	C.V.
1	89.20	10.01	0.112
2	88.86	9.87	0.111
3	87.84	10.40	0.118
4	88.83	10.64	0.120
5	89.33	11.42	0.128

Note: CV = Standard deviation/mean CT number

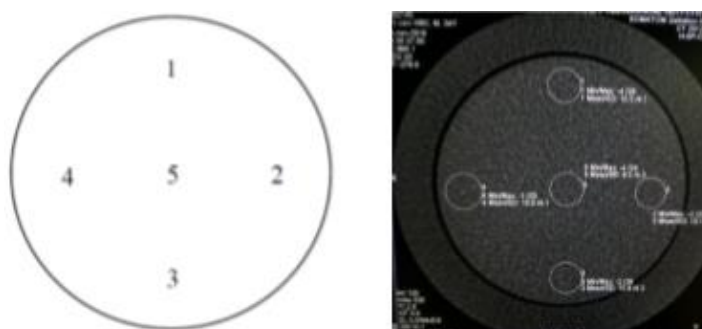


Figure I Position of ROI for CT number measurement.

Comment: Pass

Linearity of CT Numbers

Method: Set up the catphan phantom as described in beam alignment. Select the section containing the test objects of different CT numbers. Select the head technique and perform a single transverse scan. Select a region of interest (ROI) of sufficient size to cover the test objects. Place the ROI in the middle of each test object and record the mean CT number.

Technique: 120 kVp, 320 mA, 1 sec, slice collimation 5 mm. 200 mm FOV.

Tolerance: R-square between measured CT number and linear attenuation coefficient (μ) more than 0.9

Results:

Material	Expected CT no. (HU)	Measured CT no. (HU)	$\mu(\text{cm}^{-1})$
Air(inferior)	-1000	-1.013	0
Air(superior)	-1000	-1014	0
Acrylic	120	120.67	0.184
Polystyrene	-35	-36	0.162
LDPE	-100	103.91	0.151
PMP	-200	-192	0.136
Delrin	340	321	0.217
Teflon	990	905	0.305

Note: Expected CT numbers are either the predicted ones or the ones obtained during the previous annual measurement.

Comment: Pass

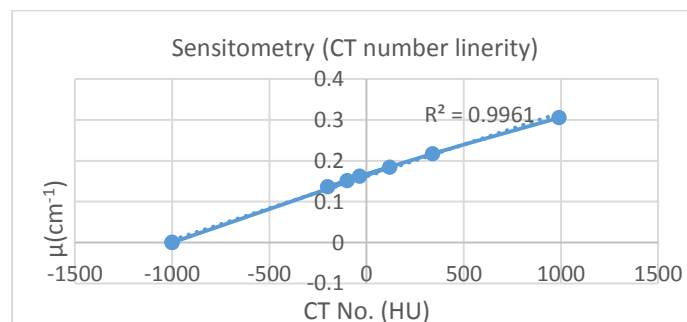


Figure II Linearity of CT number

Accuracy of Distance Measurement

Purpose: To test accuracy of Distance Measurement and for circular symmetry of the CT image.

Method: Set up the catphan phantom as described in beam alignment. Select the section containing the test accuracy of distance measurement. Select the head technique and perform a single transverse scan. Measured object in x and y axes.

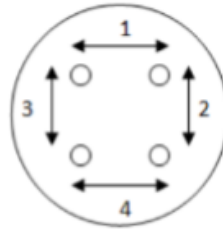


Figure III Accuracy measurement.

Results:

Position	Indicate (mm)	Measured (mm)	Different (mm)
1	50	49.3	0.7
2	50	49.3	0.7
3	50	49.1	0.9
4	50	49.2	0.8

Comment: Pass

Image uniformity

Method: Set up the catphan phantom as described in beam alignment. Select the section containing the image uniformity module. Select the head technique. Perform a single transverse scan. Measure the mean value and the corresponding standard deviations in CT numbers within a region of interest (ROI). These measurements are taken from different locations within the scan field.

Technique: 120 kVp, 300 mA, 1.0 sec, 200 mm FOV.

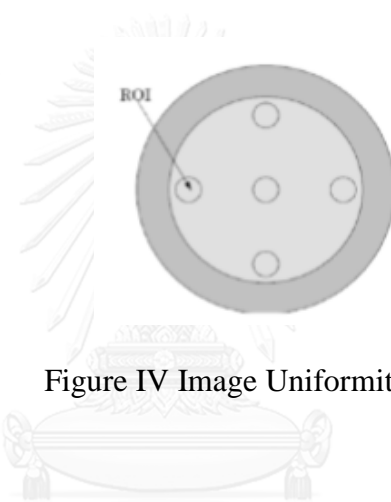


Figure IV Image Uniformity.

Tolerance: 5 HU.

Results:

Position	CT number (HU)	SD	Different (HU)
Center	3.44	10.60	0
3 o'clock	3.45	8.81	0.01
6 o'clock	4.03	8.12	0.59
9 o'clock	3.77	8.3	0.33
12 o'clock	4.94	9.16	1.5

Note: Different = |CT number center – CT number peripheral|

Comment: Pass

High Contrast Resolution

Method: Set up the catphan phantom as described in beam alignment. Select the section containing the high resolution test objects. Select the head technique. Perform a single transverse scan. Select the area containing the high resolution test objects and zoom as necessary. Select appropriate window and level for the best visualization of the test objects. Record the smallest test object visualized on the film.

Technique: 120 kVp, 300 mA, 1.0 sec, 200 mm FOV.

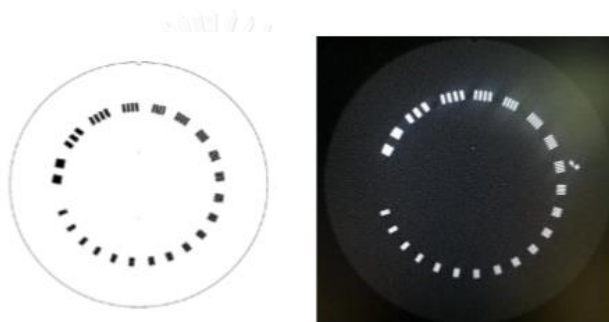


Figure V High contrast resolution.

Results:

Slice Thickness in mm	Resolution
5	11 lp/cm (0.045 mm)

Comment: Pass

Low Contrast Detectability

Method: Select the section containing the low resolution test objects in the mini phantom. Perform a single transverse scan utilizing the same technique as high resolution.

Technique: 120 kVp, 320 mA, 1.0 sec, 200 mm FOV, slice collimation 5 mm.

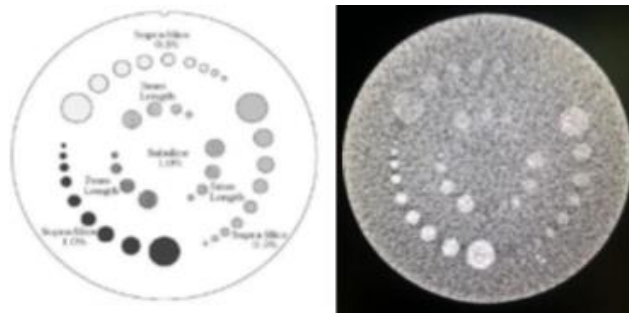


Figure VI Low contrast detectability.

Results:

Supra-slice	Nominal target contrast levels	Hole	%Contrast
	0.30%	6	1.5
	0.50%	8	1.5
	1%	9	2
Sub-slice	Nominal target contrast levels	Hole	%Contrast
	3 mm Length	4	3
	5 mm Length	4	5
	7 mm Length	4	7

Comment: Pass

Verification of Computed Tomography Dose Index (CTDI)

Purpose: To verify CTDI of scanner to the measured DLP from dosimeter.

Method: Recorded the CTDI using head protocol and scan parameter were 100 mA tube current, 1 sec scan time and kilovoltage setting of 80, 100, 120 and 135 kVp. The displayed CTDI on CT monitor were recorded to compare percentage difference with the CTDI measured values by dosimeter for each kVp.

Technique: 120 kVp, 100 mA, 1.0 sec.

Tolerance: The percent difference between the displayed CTDI on CT monitor and CTDI from measured should less the than 10%.

Results:

kVp	CTDI (mGy)		
	Displayed	Measured	% difference
80	4.91	5.7	9.7
100	9.83	10.45	5.9
120	16.22	16.94	4.3
135	24.12	24.32	0.8

Comment: Pass

Verification of Dose Length Product (DLP)

Purpose: To verify displayed DLP of scanner to the measured DLP from dosimeter.

Method: The DLP in head phantom was determined by using a 100 mm pencil ionization chamber and 16 cm diameter PMMA phantom placed at the isocenter of the CT bore. The scan parameters were 100 mA, 1 sec scan time, 200 mm FOV and 10x1 mm collimation setting for all measurements at each kVp setting of 80, 100, 120 and 135. The displayed DLP on CT monitor were recorded to compare percentage difference with the DLP measured values by dosimeter for each kVp.

Technique: 120 kVp, 100 mA, 1.0 sec, 10 mm collimation.

Tolerance: The percent difference between the displayed DLP on CT monitor and measured DLP should less the than 10%.

Results:

kVp	DLP		
	Displayed	Measured	% difference
80	9.4	9.8	4.08
100	18.9	19.5	3.08
120	31.1	32.0	2.81
135	46.3	46.6	0.64

Comment: Pass

VITA

NAME	Miss. Saiwaroon Teankuae
SEX	Female
NATIONALITY	Thai
DATE OF BIRTH	1 February 1991
PLACE OF BIRTH	Petchaburi
INSTITUTIONS ATTENDED	Mahidol University, 2009 Bachelor of Science (Radiological Technology)
POSITION HELD & OFFICE	Radiological Technologist of Department of Radiology, Phya Thai Hospital for 2 year
E-mail	saiwaroon_eye@hotmail.com